



HAL
open science

Study of the Low Temperature Oxidation of Propane

Maximilien Cord, Benoit Husson, Juan Carlos Lizardo Huerta, Olivier Herbinet, Pierre-Alexandre Glaude, René Fournet, Baptiste Sirjean, Frédérique Battin-Leclerc, Manuel Ruiz-Lopez, Zhandong Wang, et al.

► **To cite this version:**

Maximilien Cord, Benoit Husson, Juan Carlos Lizardo Huerta, Olivier Herbinet, Pierre-Alexandre Glaude, et al.. Study of the Low Temperature Oxidation of Propane. *Journal of Physical Chemistry A*, 2012, 116, pp.12214-12228. 10.1021/jp309821z . hal-00771603

HAL Id: hal-00771603

<https://hal.science/hal-00771603v1>

Submitted on 9 Jan 2013

HAL is a multi-disciplinary open access archive for the deposit and dissemination of scientific research documents, whether they are published or not. The documents may come from teaching and research institutions in France or abroad, or from public or private research centers.

L'archive ouverte pluridisciplinaire **HAL**, est destinée au dépôt et à la diffusion de documents scientifiques de niveau recherche, publiés ou non, émanant des établissements d'enseignement et de recherche français ou étrangers, des laboratoires publics ou privés.

Study of the Low Temperature Oxidation of Propane

Maximilien Cord [†], Benoit Husson [†], Juan Carlos Lizardo Huerta [†], Olivier Herbinet ^{†*}, Pierre-Alexandre Glaude [†], René Fournet [†], Baptiste Sirjean [†], Frédérique Battin-Leclerc [†], Manuel Ruiz-Lopez [‡], Zhandong Wang [§], Mingfeng Xie [§], Zhanjun Cheng [§], and Fei Qi [§]

[†] *Laboratoire Réactions et Génie des Procédés, Université de Lorraine, CNRS, ENSIC, BP 20451, 1 rue Grandville, 54000 Nancy, France*

[‡] *Laboratoire Structure et Réactivité des Systèmes Moléculaires Complexes, Université de Lorraine, CNRS, Boulevard des Aiguillettes, BP 70239, 54506 Vandœuvre-lès-Nancy, France*

[§] *National Synchrotron Radiation Laboratory, University of Science and Technology of China, Hefei, Anhui 230029, P. R. China*

Abstract

The low-temperature oxidation of propane was investigated using a jet-stirred reactor at atmospheric pressure and two methods of analysis: gas chromatography and synchrotron vacuum ultraviolet photoionization mass spectrometry (SVUV-PIMS) with direct sampling through a molecular jet. The second method allowed the identification of products, such as molecules with hydroperoxy functions, which are not stable enough to be detected by gas chromatography. Mole fractions of the reactants and reaction products were measured as a function of the temperature (530–730 K), with a particular attention to reaction products involved in the low temperature oxidation, such as cyclic ethers, aldehydes, alcohols, ketones, and hydroperoxides. A new model has been obtained from an automatically generated one, which was used as a starting point, with a large number of re-estimated thermochemical and kinetic data. The kinetic data of the most sensitive reactions, i.e., isomerizations of alkylperoxy radicals and the subsequent decompositions, have been calculated at the CBS-QB3 level of theory. The model allows a satisfactory prediction of the experimental data. A flow rate analysis has allowed highlighting the important reaction channels.

Corresponding author:

Olivier HERBINET
Laboratoire Réactions et Génie des Procédés
Ecole Nationale Supérieure des Industries Chimiques
BP 20451, 1 rue Grandville, 54000 Nancy, France
Tel: +33 (0)3 83 17 53 60
Fax: +33 (0)3 83 17 81 20
E-mail: olivier.herbinet@univ-lorraine.fr

Introduction

In contrast to larger n-alkanes,^(1,2) the low temperature oxidation of propane in the gas phase has been the subject of very few experimental studies, mainly due to its very low reactivity. This C₃ hydrocarbon is not very reactive because of the short size of the alkyl chain which limits the low temperature branching paths. Therefore, conditions which are required to observe some reactivity for propane are close to the domain of explosion.

Vogin et al.⁽²⁾ studied the oxidation of propane in a closed vessel at the temperature of 623 K and at subatmospheric pressures (initial pressure of 125 Torr) for equimolar mixtures of propane and oxygen ($\phi = 5$). They recorded the evolution of the partial pressures of reaction products as a function of reaction time. They observed the formation of numerous reaction products: hydrocarbons such as methane, ethylene, propene, and oxygenated species such as carbon oxides, formaldehyde, methanol, acetaldehyde, methyloxirane, oxetane, acetone, propanal, and hydrogen peroxide. The authors proposed some routes for the formation of the main reaction products.

More recently, Koert et al.⁽³⁾ studied the oxidation of lean and diluted propane-oxygen mixtures through the negative temperature coefficient region in a plug flow reactor at pressures ranging from 2 to 15 atm. They showed that propane was reactive from 675 K with a strong negative temperature coefficient in the range 750 - 775 K. They detected and quantified many reaction products by gas chromatography, the main ones being carbon oxides, ethylene, propene, formaldehyde, and acetaldehyde. They also observed the formation of minor species such as acetone, propanal, propylene oxide (methyloxirane), acrolein, methanol, and n-butane.

In the purpose of reinvestigating the low temperature oxidation of propane in the light of the recent new kinetic knowledge gained for light alkanes^(4,5) and alkenes,⁽⁶⁾ this study presents new experimental results for the oxidation of propane in a jet-stirred reactor, as well as a new model largely based on quantum calculations. To widen the range of analyzed species, two different analytical methods have been used: online gas chromatography (GC) (experiments made in Nancy, France) and synchrotron vacuum ultraviolet photoionization mass spectrometry (SVUV-PIMS) with direct sampling through a molecular jet (experiments made in Hefei, China). The advantage of the second method is that reactive species, such as branching agents, are frozen in the molecular jet and can be detected in the mass spectrometer, whereas this type of species would have already decomposed before the injection in a gas chromatograph.⁽⁷⁾ But a major disadvantage of this technique is the difficulty to distinguish between the different isomers (as the signal is the sum of all species having the same mass) when their ionization energies are close. Another difficulty is the quantification of species with unknown cross sections. Both techniques appear to be fully complementary since the identification of isomers is relatively easy in gas chromatography coupled to mass spectrometry.

Experimental Method

The oxidation of propane was performed in a jet-stirred reactor which can be modeled as a perfectly stirred reactor.⁽⁸⁾ This type of reactor has often been used for gas phase kinetic studies (e.g., refs 9–11). Experiments were performed at a constant pressure of 1.06 bar, at a residence time of 6 s, at temperatures ranging from 550 to 730 K, under stoichiometric conditions and the fuel was diluted in an inert gas. Note that due to the low reactivity of this hydrocarbon under these conditions, a particularly large mole fraction of propane (0.12) had to be used. The inert gas was helium in Nancy and argon in Hefei. The use of argon was required in Hefei because its signal at an ionization energy of 16.6 eV is used for the normalization of the signals of other peaks. Gases used in Nancy were provided by Messer with purities of 99.999, 99.995 and 99.95% for helium, oxygen and propane, respectively. In China, gases were provided by Nanjing Special Gas Factory Co., Ltd. Purities were 99.99, 99.999 and 99+% for argon, oxygen and propane, respectively.

The reactor, made of fused silica, consists of a quartz sphere (volume = 95 cm³) into which the diluted reactant enters through an injection cross located at its center. The reactor was operated at constant temperature and pressure and it was preceded by an annular preheating zone in which the temperature of the gases was increased up to the reaction temperature before entering inside the reactor. Gas mixture residence time inside the annular preheating was very short compared to the residence time inside the reactor (a few percent). In Nancy, both the spherical reactor and the annular preheating zone were heated by Thermocoax heating resistances rolled up around their walls. In Hefei, because of the lateral cone connecting the reactor to the mass spectrometer, it was difficult to use heating resistances for the heating of the spherical part.⁽⁷⁾ A special oven with the shape of the reactor (sphere and cone) was designed and used for the heating. The accuracy of the temperature with the two types of heating device is ± 5 K. Gas flow rates for the feed of the reactor were controlled by mass flow controllers provided by Bronkhorst for the experiments in Nancy and by mass flow controllers provided by MKS and Bronkhorst in Hefei. The error in the flow measurements is around 1% for each controller. This results in a maximum error of about 2% in the residence time.

Analytic Method (Nancy)

The outlet species were analyzed online by gas chromatography. The online analysis of products which are liquid under standard conditions was enabled by a heated transfer line connecting the reactor outlet and the chromatograph sampling gate which was also heated. The temperature of the transfer line can be set at our convenience between ambient temperature and 473 K maximum. During the propane study, the temperature of the transfer line was set at 423 K and sufficiently low to avoid thermal reaction in the line. This temperature is high enough to keep all the reaction products in the gas phase. Two gas chromatographs were used for the quantification of the different species.

The first gas chromatograph, equipped with a Carbosphere-packed column, a thermal conductivity detector (TCD), and a flame ionization detector (FID), was used for the quantification of O₂, CO, CO₂, methane, ethylene, acetylene and ethane. The second one was fitted with a PlotQ capillary column and a FID. It was used for the quantification of molecules from methane to reaction products with up

to 5 carbon atoms and 1 or 2 oxygen atoms maximum. Maximum relative errors in mole fractions are estimated to $\pm 10\%$, and the limit of detection for species is about 1 ppm for species analyzed using flame ionization detector and 100 ppm for species analyzed using thermal conductivity detector.

The identification of reactions products, which were not calibrated before, was performed by thermodesorption (after a beforehand sorption of the outlet gas reactor on Tenax TA adsorbent) coupled with a gas chromatograph equipped with a PlotQ capillary column and a mass spectrometer. The mass spectra of all detected reaction products were available in the NIST 08 mass spectral library making the identification work relatively simple.

Analytic Method (Hefei)

Species from the reactor were analyzed by a reflectron time-of-flight mass spectrometer with photoionization by synchrotron radiation. The reactor was coupled to the low pressure photoionization chamber through a lateral fused silica cone-like nozzle which was inserted in the spherical part. The tip of the cone was pierced by a 50 μm orifice. A nickel skimmer with a 1.25 mm diameter aperture was located 15 mm downstream from the sampling nozzle. The sampled gases formed a molecular beam, which was passed horizontally through the 10 mm gap between the repeller and extractor plates of the RTOF MS. The molecular beam was intersected perpendicularly with synchrotron vacuum ultraviolet light beam. The ion signal was then detected with a RTOF MS, which was installed in the photoionization chamber vertically. Additional details about this experimental apparatus are available in previous work.⁽⁷⁾

The experiments performed in France (gas chromatographic analyses) have been repeated in China (SVUV-PIMS) under exactly the same conditions. Some species were detected in both studies and mole fractions of some of them were compared to check the consistency between both sets of experiments. Mole fractions of some reaction products which were not detected using gas chromatography (water, hydrogen peroxide and formaldehyde) have been only calculated using the experimental data obtained using SVUV-PIMS.

Experimental Results

Hereafter are presented both sets of experimental data obtained in Nancy and in Hefei, respectively.

Analyses Using Gas Chromatography (Nancy)

The mole fraction profiles of propane and oxygen are displayed in Figure 1. Under the conditions of this study, propane is not very reactive: the reaction starts lately around 613 K and the conversion only reaches 20% in the temperature range 625 - 650 K. The reactivity becomes very low in the negative temperature coefficient zone (650 - 700 K) and slightly rises again around 725 K. No investigation was performed at higher temperature to avoid explosion due to the very high concentration of fuel. As shown in Table 1, 21 one reaction products (plus the two reactants) were detected and quantified in this study. Their mole fraction profiles are displayed in Figures 1 and 2.

These reaction products are hydrocarbons, and oxygenated species having one, two or three carbon atoms. Species with one or two carbon atoms are carbon monoxide, methane, ethylene, oxirane, acetaldehyde, methanol, and acetic acid. Note that a large peak of formic acid is shown by GC-MS but cannot be quantified by FID. C₃ species are: propene, methyloxirane, oxetane, propanal, acetone, acrolein, *n*-propanol, 2-propanol, 2-propen-1-ol, and 1-hydroxy-2-propanone. All these species are observed above 613 K, i.e., from the temperature at which the reaction starts. Note that 1-hydroxy-2-propanone has a very different mass spectrum compared to the other compounds of the same mass which could have been envisaged according to the kinetic model (see later in the text), e.g. 3-hydroxypropanal and saturated C₃ hydroxyl cyclic ethers.

Table 1. List of Species Detected Using Gas Chromatography and SVUV-PIMS^a

Name	Molecular formula	m/z	Ionization energy (eV)	Quantification using gas chromatography	Quantification using SVUV-PIMS	Maximum mole fraction ^(b)
Methane	CH ₄	16	12.61	×		4.14×10 ⁻⁵
Water	H ₂ O	18	12.62		×	4.38×10 ⁻²
Ethylene	C ₂ H ₄	28	10.51	×		1.27×10 ⁻³
Carbon monoxide	CO		14.01	×		1.36×10 ⁻²
Formaldehyde	CH ₂ O	30	10.88		×	3.08×10 ⁻²
Methanol	CH ₄ O	32	10.84	×		4.61×10 ⁻³
Oxygen (reactant)	O ₂		12.07	×	×	–
Hydrogen peroxide	H ₂ O ₂	34	10.58		×	2.55×10 ^{-2(e)}
Propene	C ₃ H ₆	42	9.73	×	×	7.37×10 ⁻³
Acetaldehyde	C ₂ H ₄ O		10.23	×		3.47×10 ⁻³
Oxirane	C ₂ H ₄ O	44	10.56	×		3.76×10 ⁻⁴
Propane (reactant)	C ₃ H ₈		10.94	×	×	–
Acrolein	C ₃ H ₄ O	56	10.11	×		3.96×10 ⁻⁵
Oxetane	C ₃ H ₆ O		9.65	×		1.18×10 ⁻⁴
2-Propen-1-ol	C ₃ H ₆ O		9.67	×		7.83×10 ⁻⁵
Acetone	C ₃ H ₆ O	58	9.70	×		2.03×10 ⁻⁴
Propanal	C ₃ H ₆ O		9.96	×		3.79×10 ⁻⁵
Methyloxirane	C ₃ H ₆ O		10.22	×		5.61×10 ⁻⁴
<i>iso</i> -Propanol	C ₃ H ₈ O		10.17	×		6.96×10 ⁻⁵
<i>n</i> -Propanol	C ₃ H ₈ O	60	10.22	×		4.15×10 ⁻⁵
Acetic acid	C ₂ H ₄ O ₂		10.65	×	×	1.35×10 ⁻⁴
1-Hydroxy-2-propanone	C ₃ H ₆ O ₂	74	10.00	×		1.08×10 ⁻⁴
Propyl-hydroperoxide isomers	C ₃ H ₈ O ₂	76	9.42-9.50 ^(a)		×	^(d)

^a Ionization energies come from the NIST WebBook.(12).

^b Ionization energies calculated in this study (see Table 2).

^c When the species was quantified using both methods, the maximum mole fraction is the one obtained using gas chromatography.

^d The cross section of this species was unknown. A value of 10 Mb was used for the quantification.

^e Propyl hydroperoxide isomers could not be quantified due to the lack of data concerning their cross sections.

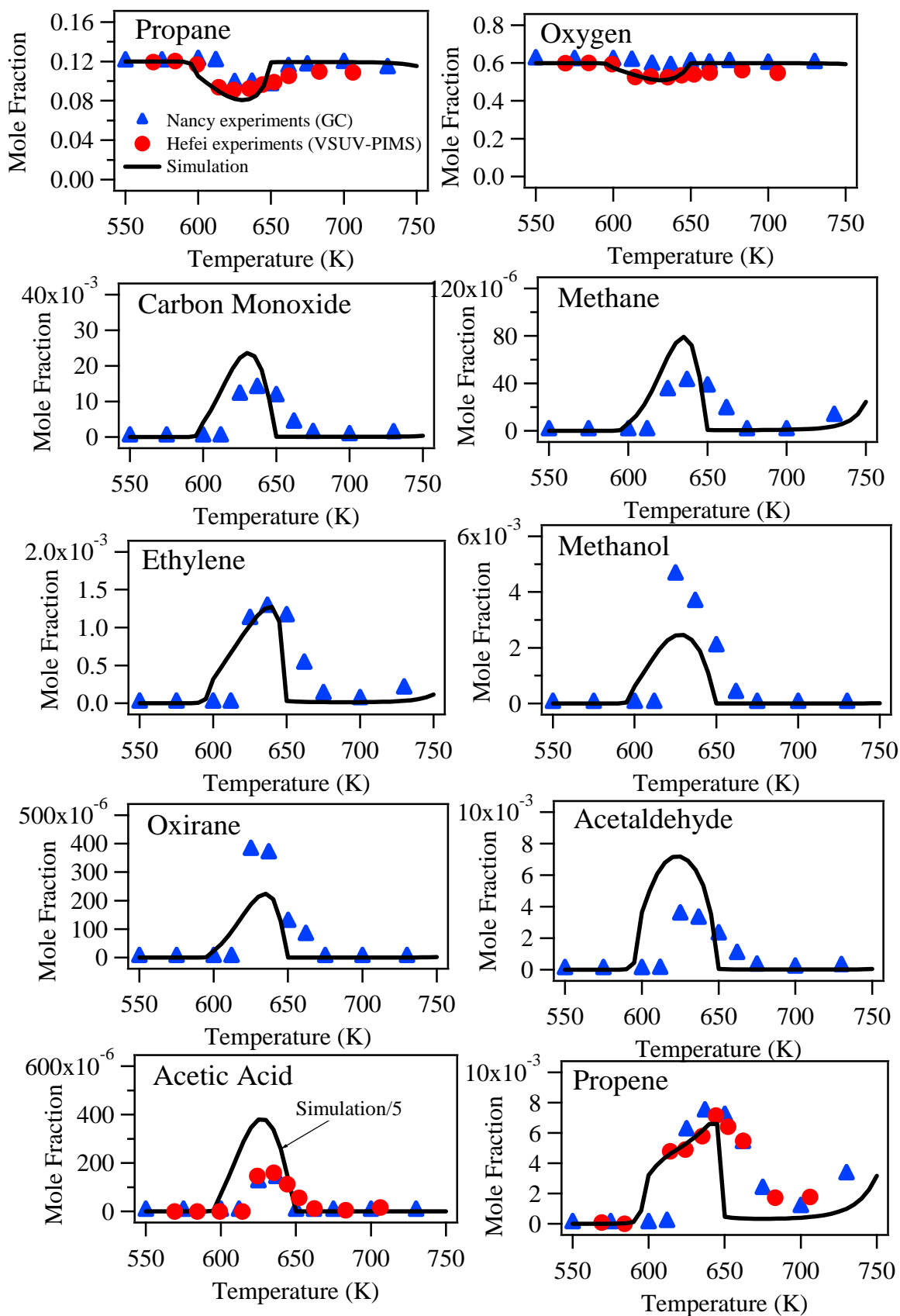


Figure 1. Mole fraction profiles of propane, oxygen, reaction products having up to two carbon atoms, and propene (stoichiometric mixture; residence time = 6 s).

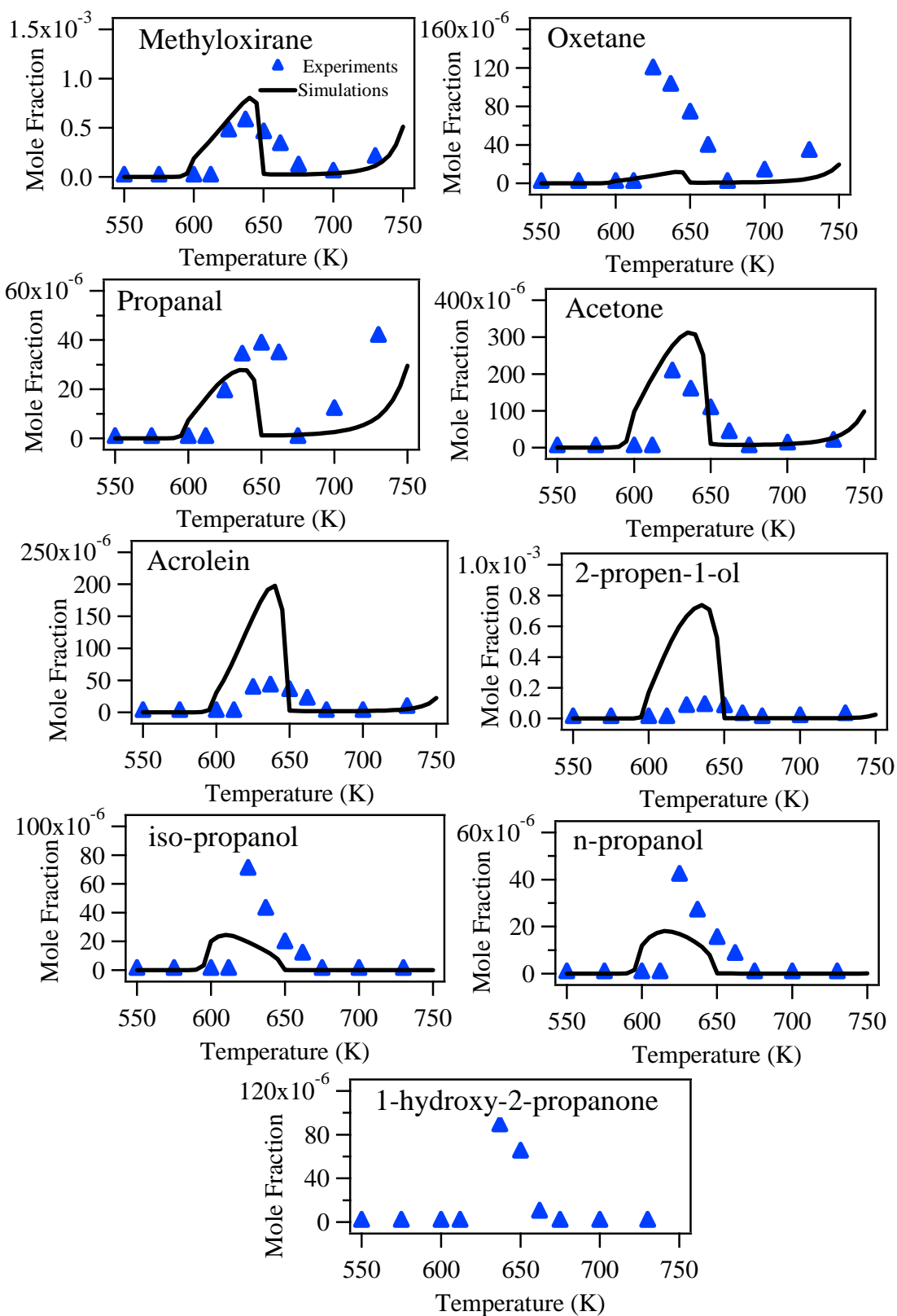


Figure 2. Mole fraction profiles of oxygenated C₃ oxidation products (stoichiometric mixture; residence time = 6 s).

Some differences are visible in the mole fraction profiles of these species. For some of them (e.g., methanol or acetone), the mole fraction increases sharply at 625 K and then decreases in a monotonous way up to 675 K. For some others, the mole fraction increases more smoothly before passing through a maximum and then decreasing (e.g., carbon monoxide or methane).

Analyses Using SVUV-PIMS (Hefei)

The experiments performed in Nancy were repeated in Hefei under the same conditions. The data obtained using SVUV-PIMS have been used to identify the reaction products from their ionization energies and to obtain mole fraction profiles. A few species could not be quantified because of a lack of data of photoionization cross sections.

- Identification of the Species

Figure 3 displays a mass spectrum obtained at 635 K (corresponding to the temperature range where the reactivity is highest) and at a photon energy of 11.00 eV. Under these conditions, the main peaks are obtained for m/z 30, 42, and 44. The identification of the species that correspond to the detected m/z was obtained using photoionization efficiency spectrum shown in Figure 4 (the scan in energy was made from 9.43 to 11.70 eV). The larger signals correspond to the following masses:

- m/z 30: the peak likely corresponds to formaldehyde (ionization energy (IE) of 10.88 eV⁽¹²⁾).
- m/z 42: the peak is likely for propene (IE of 9.73 eV⁽¹²⁾).
- m/z 44: the peak corresponds to acetaldehyde (IE of 10.23 eV⁽¹²⁾) and oxirane (IE of 10.56 eV⁽¹²⁾). At photon energies larger than 11.00 eV, the peak at m/z 44 is also for propane (the reactant) which has an IE of 10.94 eV according to the literature.⁽¹²⁾

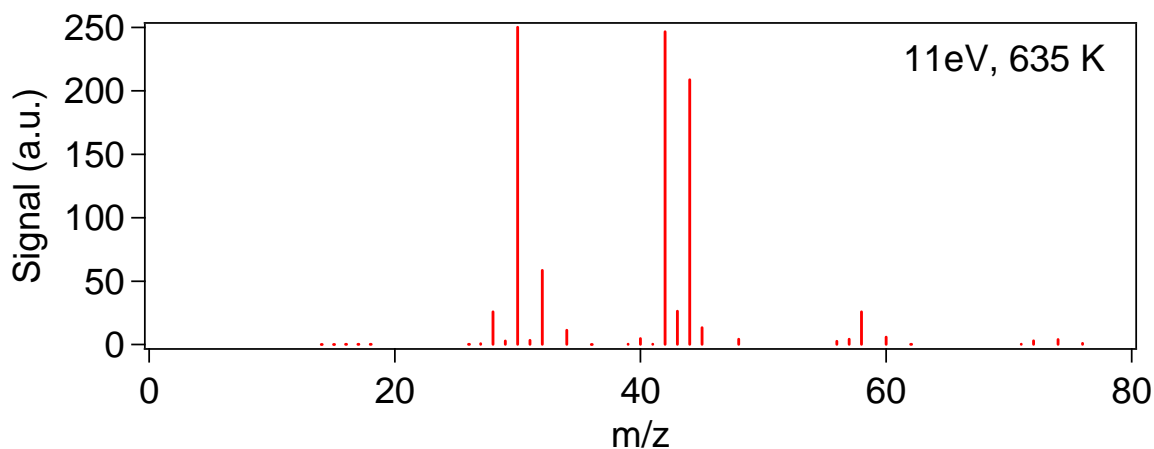


Figure 3. Mass spectrum obtained at a photoionization energy of 11 eV and at a temperature of 635 K.

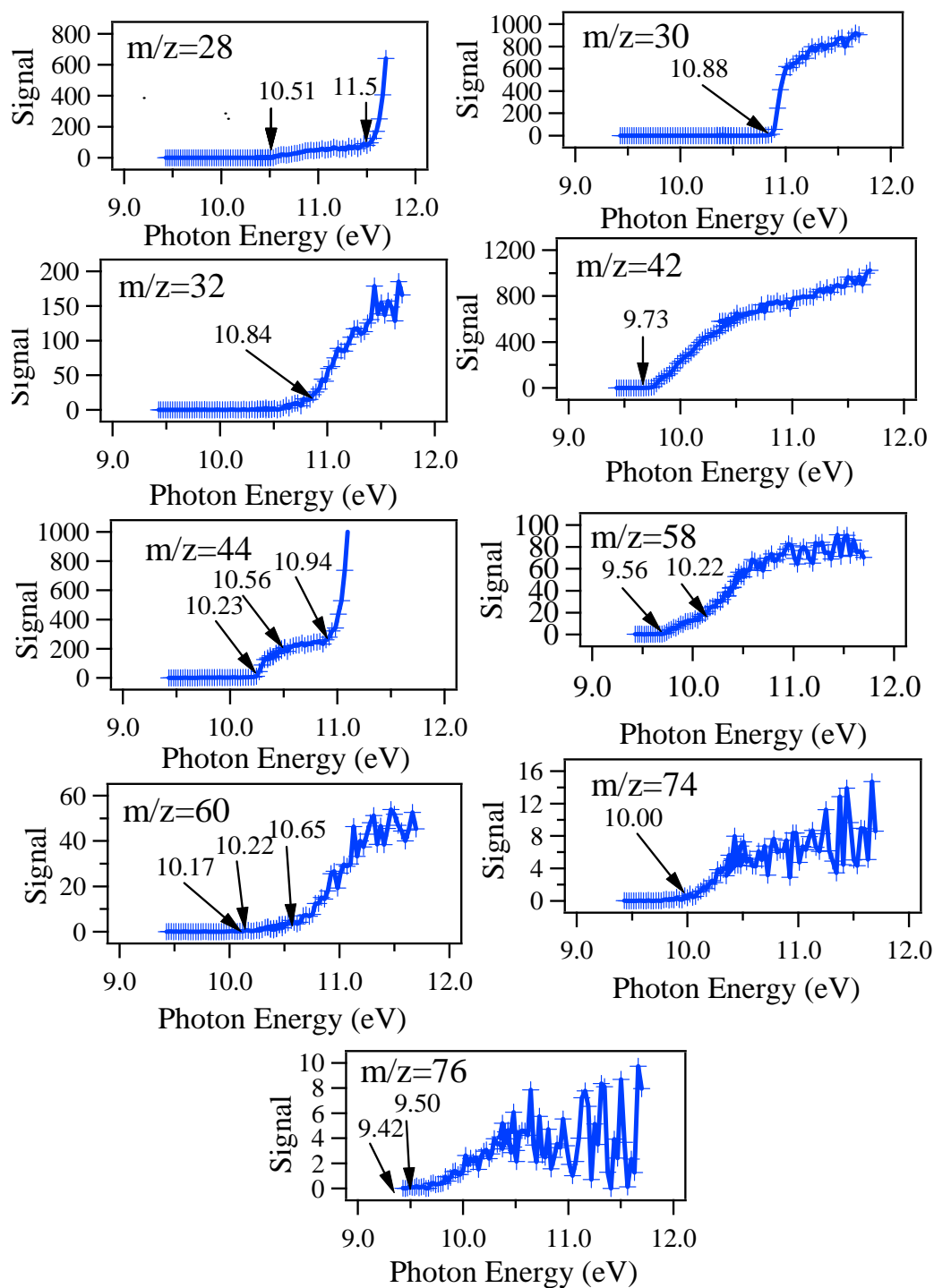


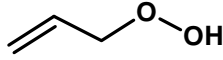
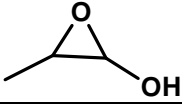
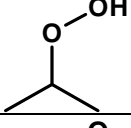

Figure 4. Photoionization efficiency spectra of mass 30, 42, 44, 58, 60, 74, and 76 for a reaction temperature of 630 K. Signals are in arbitrary units. For masses 30 to 60, the numbers given in graphs are ionization energies (in eV) taken from the NIST Webbook⁽¹²⁾ for the species of Table 1; for masses 74 and 76, calculated values (see text) are displayed.

Smaller peaks were detected for m/z 28, 32, 58, 60, 74, and 76:

- m/z 28: the peak corresponds to ethylene (IE of 10.51 eV⁽¹²⁾) and to carbon monoxide which has the same mass, but an IE of 14.01 eV.⁽¹²⁾ The large increase in the signal around 11.50 eV likely corresponds to the $C_2H_4^+$ fragment from propane. The large contribution of this fragment masked the contribution of carbon monoxide (at photoionization greater than 14.01 eV) making a precise quantification of this species impossible here.
- m/z 32: this corresponds to methanol (IE of 10.84 eV⁽¹²⁾). This m/z also corresponds to oxygen molecule but the IE is much higher (IE of 12.07 eV⁽¹²⁾).
- m/z 58: this peak is for several isomers with the formula C_3H_6O : acetone, propanal, oxetane, methyloxirane, and 2-propen-1-ol. All these species are present in similar amounts and have a very close IE (9.70, 9.96, 9.65, 10.22, and 9.67, respectively⁽¹²⁾). The scan for m/z 58 (Figure 4) shows that the signal starts increasing at about 9.70 eV, which is consistent with the IE of oxetane, acetone, and 2-propen-1-ol.
- m/z 60: this likely corresponds to acetic acid, n-propanol and 2-propanol (IE of 10.65, 10.22 and 10.17, respectively⁽¹²⁾).
- m/z 74: there are several possible $C_3H_6O_2$ isomers. According to the photoionization efficiency spectra for m/z 74 (Figure 4), the signal starts increasing from 10.00 eV. This value is not in agreement with the ionization energies of propanoic acid (10.44 eV⁽¹²⁾), allylhydroperoxide (9.52 eV) and 2,3-methyl,hydroxyl-oxirane (8.79 eV). Note that ionization energies of allylhydroperoxide and 2,3-methyl,hydroxyl-oxirane were not available in the literature and were calculated theoretically. Table 2 presents zero-point energy corrected adiabatic ionization energies (AIE) calculated from the composite CBS-QB3 method⁽¹³⁾ using Gaussian09.⁽¹⁴⁾ For each species, geometry optimization, at the B3LYP/cbsb7 level of theory was performed for the molecule and the corresponding cation. From these optimized geometries, an energy calculation, at the CBS-QB3 level, was done at 0 K, both for molecule and cation. Zero point energy (ZPE) was added to the previous energies and the AIE was obtained from the difference between these two quantities. The precision of the ionization energies calculated with this method is ± 0.09 eV. Contrary to the ionization threshold of the isomers cited above, the experimental ionization energy of m/z 74 seems to be in good agreement with that of 1-hydroxy-2-propanone (10.0 ± 0.1 eV⁽¹⁵⁾), which was also detected in the gas chromatography analyses.
- m/z 76: this peak likely corresponds to hydroperoxide species with the formula $C_3H_8O_2$ (Table 2). There are no data about their IE in the literature and calculations were performed using the same method as for the two $C_3H_6O_2$ isomers. The calculated IEs are 9.42 and 9.50 eV for isopropyl-hydroperoxide and propyl-hydroperoxide, respectively. No conclusion can be given about isopropyl-hydroperoxide since the calculated IE is below the energy at which our scan has been started. However there is a very good agreement between the calculated and the experimental value (9.49 eV, see Figure 4) for propyl-hydroperoxide. We will nevertheless consider the peak at m/z 76 as due to the sum of both isomers.

Note that, contrary to our previous work for larger alkanes (n-butane,(7)n-heptane⁽¹¹⁾), it has not been possible to detect ketohydroperoxides (m/z 90).

Table 2. Ionization Energies of Two C₃H₆O₂ Isomers (m/z 74) and of C₃H₈O₂ Hydroperoxides (m/z 76) Calculated at the CBS-QB3 Level of Theory (Uncertainty of Calculated Ionization Energies Is ±0.09 eV)

m/z	Name	Structure	Calculated ionization energy (eV)
74	allyl-hydroperoxide		9.52
	2,3-methyl,hydroxy-oxirane		8.79
76	isopropyl-hydroperoxide		9.42
	propyl-hydroperoxide		9.50

- Quantification of the Species

The quantification of reaction products was performed for the reactants (propane and oxygen), propene, acetic acid, water, hydrogen peroxide, and formaldehyde (the last three species were not detected by GC). For the quantification of all these species, we used the normalized signal (i.e., the signal which was normalized by the one of argon at 16.60 eV to take into account the change in total flow rate and the reaction temperature effect on the sampling). For propane and oxygen (Figure 1), the inlet mole fractions were known and the calibration was performed assuming no reaction at 575 K. Then the mole fractions of the reaction products were calculated using the following equation:

$$x_i(T) = x_{ref}(T) \times \frac{S_i(T)}{S_{ref}(T)} \times \frac{\sigma_{ref}(E)}{\sigma_i(E)} \times \frac{D_{ref}}{D_i} \quad (1)$$

$x_i(T)$ and $S_i(T)$ are the mole fraction and the signal of a species i at the temperature T , respectively. $\sigma_i(E)$ is the photoionization cross-section of the species i at the photon energy E . D_i is the mass discrimination factor of species i .

The mole fraction of propene was calculated from the propane data at 13.00 eV in order to compare with the mole fractions obtained using gas chromatography. Cross sections of propane and propene at 13.00 eV were estimated as 15.11 Mb⁽¹⁶⁾ and 25.21 Mb⁽¹⁷⁾ respectively. Figure 1 displays both sets of propene mole fractions, showing a very good agreement between both experimental sets.

Mole fractions of water, hydrogen peroxide, and formaldehyde (not quantified in Nancy) were calculated using the same procedure using the signals at 13.00 eV. The cross sections used for the quantification of water and formaldehyde are from Katayama et al.,⁽¹⁸⁾ and Cooper et al.,⁽¹⁹⁾ respectively. As far as hydrogen peroxide is concerned, there is no cross section data available. However as in our previous work on n-butane,⁽⁷⁾ an arbitrary value of 10.00 Mb was used for the calculation. The mole fraction profiles of these species are displayed in Figure 5.

Acetic acid was quantified using the signal of ethylene as a reference. Signals obtained at 11 eV were used for the quantification. Cross sections of acetic acid and ethylene at 11.00 eV were 7.56 Mb⁽¹¹⁾

and 7.48 Mb,⁽²⁰⁾ respectively. The mole fraction profile of acetic acid is displayed in Figure 1. Note that there is a good agreement between measurements made by GC with FID and by SVUV-PIMS. Figure 5 also displays the signal obtained for an energy of 11.00 eV at m/z 76, i.e. for C₃ propyl hydroperoxides. In this case, due to absence of photoionization cross sections, the quantification was not possible.

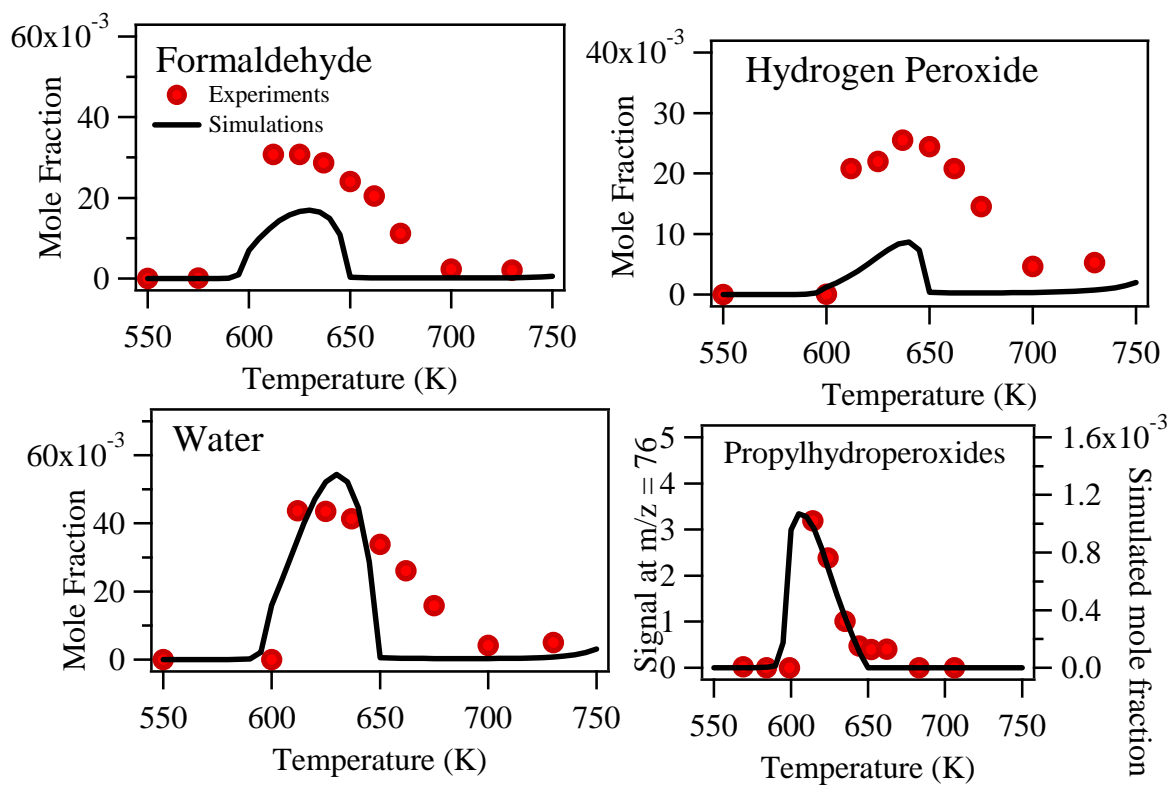


Figure 5. Mole fraction profiles of propane oxidation products that were quantified only using SVUV photoionization mass spectrometry and signal at $m/z = 76$ obtained at 11 eV (stoichiometric mixture; residence time = 6 s).

Model Development for the Oxidation of Propane

As in our previous work about the oxidation of n-butane,⁽⁵⁾ a model generated using the EXGAS software which has already been extensively described in the case of alkanes (e.g., refs 21 and 22), and alkenes^(23,24) has been used as a basis for a model of the oxidation of propane. The generic reactions used in EXGAS are derived from the current understanding of the low-temperature oxidation of alkanes⁽²⁵⁻²⁷⁾ and alkenes^(1,26). However, in the case of several classes of reaction the thermochemical and kinetic parameters have been revised using calculations based on quantum methods (see method description hereafter). As propene is the most important C₃ product of the oxidation of propane, the mechanism has been generated considering as the initial reactants both propane and propene. In the next paragraphs, after a reminder on the specificities of the low temperature oxidation chemistry of alkanes and alkenes, we will describe, first the mechanism proposed for propane, then that of propene, and finally the thermochemical data and reactions of C₀-C₂ species.

Theoretical Calculations

This part describes the method used to perform the theoretical calculations the results of which are presented further in the text. The calculations of thermochemical data for molecules, radicals, and transition states were performed at the CBS-QB3 level of theory⁽¹³⁾ implemented in Gaussian 09 Rev. B.01.⁽¹⁴⁾ For each species considered, the conformer with the lowest energy has been identified, by performing relaxed scans, in particular for radicals which involve hydrogen bonding. Intrinsic reaction coordinates (IRC) calculations have been done at the B3LYP/cbsb7 level of theory to ensure that the transition states correctly connect the reactants and the products. Enthalpies of formation at 298 K have been obtained from isodesmic reactions. For vibrational partition function, Q_{vib}, the harmonic oscillator approximation has been assumed, except for low frequency vibrations which correspond to internal rotations. In these latter cases, a hindered rotor treatment was used. The rotational barriers have been estimated by relaxed scans at the B3LYP/cbsb7 level of theory and have been used to correct Q_{vib} from Pitzer and Gwinn tabulations.⁽²⁸⁾ For transition states, we have used the same procedure, but by freezing the atoms involved in the reaction coordinate (i.e., the cyclic part of the transition states for isomerizations), and by taking into account the remaining torsions. Reduced moments of inertia for internal rotations as well as thermochemical properties as a function of temperature have been calculated using the ChemRate software⁽²⁹⁾ according to statistical mechanical principles.

High pressure limit rate constants were calculated with the software ChemRate,⁽²⁹⁾ using canonical transition state theory (TST):

$$k_{\infty} = rpd \kappa(T) \frac{k_b T}{h} \exp\left(-\frac{\Delta G^{\ddagger}(T)}{RT}\right)$$

where ΔG^{\ddagger} is the Gibbs energy of activation, rpd the reaction path degeneracy, and $\kappa(T)$ the transmission coefficient. Tunneling effects were taken into account for internal hydrogen atom transfers. Transmission coefficients were calculated following the Eckart-1D method.⁽³⁰⁾ The kinetic

parameters were obtained by fitting the rate constant values obtained from TST at several temperatures between 500 and 1200 K, using the modified-Arrhenius expression:

$$k_{\infty} = AT^n \exp\left(-\frac{E}{RT}\right)$$

Low Temperature Oxidation of Alkanes and Alkenes

Except from resonance stabilized allylic (e.g., allyl, C₃H₅) radicals, which are obtained from alkenes by H-abstraction and have a low reactivity with a predominance of termination reactions,⁽¹⁾ the most important type of radicals involved in the oxidation of alkanes and alkenes are alkylic radicals. At low temperature, i.e. below 900 K, alkylic radicals (R•) are produced by H-abstraction from alkanes mostly by •OH radical, or by addition of •OH radical to the double bond of an alkene. Figure 6 shows a simplified scheme of the reactions with oxygen which are now usually included in models in the case of alkylic radicals (R•).⁽²⁶⁾ Alkyl radicals add thereafter to O₂ and yield peroxy radicals ROO•. Some consecutive steps then lead to the formation of hydroperoxides, which are degenerate branching agents explaining the high reactivity of alkanes at low temperatures. Alkylhydroperoxides can be directly obtained by reaction of ROO• radicals with a •HO₂ radical. In another pathway, ROO• radicals first isomerize to give hydroperoxyalkyl radicals (•QOOH). This first isomerization, which occurs via an intramolecular H-abstraction through a cyclic transition state, has a very large influence on the low-temperature oxidation chemistry. According to the size of the cyclic ring involved in the transition state, the formation of the conjugated alkene or alkenol can compete with the isomerization, mainly, at low temperature, by a direct elimination of •HO₂ from ROO•. For hydroxyalkyl radicals, the isomerizations of •QOOH radicals can also occur through the Waddington mechanism shown in Figure 7⁽³¹⁾ and lead to the formation of aldehydes (formaldehyde and acetaldehyde in the case of radicals deriving from propene) and •OH radicals. This type of reaction does not lead to the formation of branching agents and is then one of the causes of the lower reactivity of alkenes compared to alkanes.

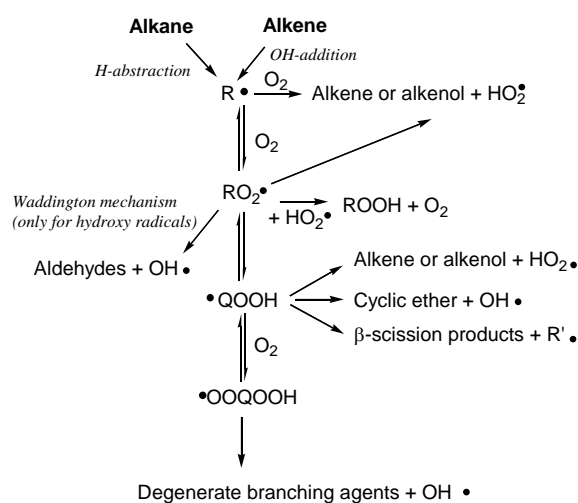


Figure 6. Simplified scheme of the reactions with oxygen which are now usually included in models in the case of alkylic radicals (R•). R• can be either an alkyl radical or an hydroxyalkyl radical.

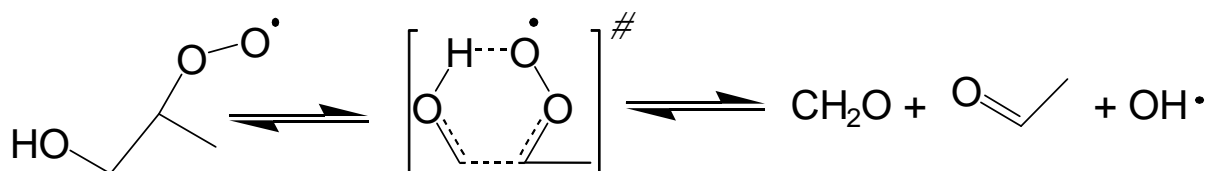
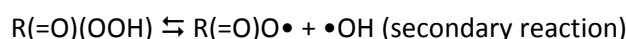
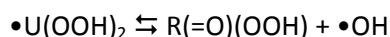


Figure 7. Isomerization of 1-hydroxy-2-propylperoxy radicals according to the mechanism of Waddington.⁽²⁸⁾

•QOOH radicals can thereafter add on O₂ and yield •OOQOOH radicals that react by a second internal isomerization producing •U(OOH)₂ radicals. The rapid unimolecular decomposition of •U(OOH)₂ radicals leads to one radical and a degenerate branching agent (keto-hydroperoxide), which is the source of the chain branching occurring at low temperatures:



In this scheme, a •OH radical reacting by H-abstraction with the initial alkane leads to the formation of three free radicals, two •OH and a R(=O)O• radical. This autoaccelerating process strongly promotes the oxidation of alkanes below 700 K. If the Waddington mechanism is not the main fate of the involved hydroxy radicals, a •OH radical adding to the double bond of an alkene can be the cause of a radical multiplication and of an accelerating effect.

When the temperature increases, the equilibrium $\text{R}\bullet + \text{O}_2 \rightleftharpoons \text{ROO}\bullet$ begins to be displaced back to the reactants and the formation of ROO• radicals is less favored compared to the strongly inhibiting oxidation reaction $\text{R}\bullet + \text{O}_2 \rightleftharpoons \bullet\text{HO}_2 + \text{conjugated alkene or alkenol}$. This reaction is equivalent to a termination step since •HO₂ radicals react mostly by disproportionation ($2\bullet\text{HO}_2 \rightleftharpoons \text{H}_2\text{O}_2 + \text{O}_2$). Unimolecular decompositions of •QOOH radicals compete with O₂ addition: •QOOH radicals can decompose into cyclic ethers or ketones and •OH radicals, or by β-scission into •HO₂ radicals and conjugated unsaturated molecules or smaller species. Because of the decrease in the production of hydroperoxides, the reactivity decreases in the 700 to 800 K temperature range. This temperature region is consequently called the negative temperature coefficient (NTC) zone. At higher temperatures, the decomposition of H₂O₂ ($\text{H}_2\text{O}_2 (+\text{M}) \rightleftharpoons 2\bullet\text{OH} (+\text{M})$) is a new source of the chain branching leading to an increase of the reactivity. This reaction becomes very fast above 900 K. NTC behaviors are usually less pronounced in the cases of alkenes than for alkanes but can nevertheless still be observed.^(23,24)

Primary and Secondary Mechanism of the Oxidation of Propane

The mechanism generated by EXGAS for the oxidation of propane contains unimolecular and bimolecular initiations, as well as H-abstractions producing propyl radicals with kinetic data proposed by Buda et al.⁽²²⁾ This mechanism also includes the reactions of propyl radicals with oxygen, which are of particular importance at low temperature, as well as the subsequent reactions of propylperoxy radicals. The current understanding of these reactions for small alkyl radicals, such as ethyl or propyl radicals, is in agreement with the fact that the $\text{R}\bullet + \text{O}_2$ reaction proceeds through a barrierless addition pathway to form the chemically activated ROO* adduct, which can either be stabilized or

react via a concerted elimination of $\bullet\text{HO}_2$ to give the conjugated alkene.⁽³²⁾ Combining theoretical calculations with an experimental investigation of the time-resolved formation of $\bullet\text{OH}$, DeSain et al.⁽⁴⁾ reported kinetic parameters for the different possible channels at different pressures in the case of propyl radicals. We have then used the values proposed under 1 atm for all the reactions of oxygen with propyl radicals. In the case of the addition to oxygen of hydroperoxypropyl radicals, the kinetic parameters have been derived from the values proposed by DeSain et al.⁽⁴⁾ for propyl radicals just considering whether the radical was primary or secondary.

The rate constants for the isomerizations of propylperoxy radicals involving a cyclic transition state including five or six atoms, as well as the formation of cyclic ethers (methyloxirane and oxetane) have been estimated as described by Cord et al.⁽⁵⁾ and deduced from CBS-QB3 quantum chemical calculations for n-butane oxidation.⁽¹³⁾

Since the number of possible isomerizations of C_3 peroxy radicals is more limited than for larger radicals, we have considered not only the isomerizations involving a transition state including five or six atoms, but also those with a four-membered transition state, with the kinetic data proposed by Buda et al.⁽²²⁾ These isomerizations are usually neglected in the mechanism proposed for the oxidation of larger alkanes. The product of this isomerization is a α -hydroperoxyalkyl radical which has been shown to be unstable or metastable.⁽³³⁾ A global step involving the isomerization and the decomposition of the obtained $\bullet\text{QOOH}$ radical by the β -scission of the O–O bond has then been written yielding $\bullet\text{OH}$ radical and acetone or propanal. The correlations performed by Cord et al.⁽⁵⁾ have also been used to estimate the rates constant of the globalized reactions of isomerization/decomposition from hydroperoxypropylperoxy radicals yielding ketohydroperoxides.

The mechanism generated by EXGAS for propane also includes all the possible β -scission reactions of all the radicals obtained by oxygen additions and isomerization with kinetic data proposed by Buda et al.⁽²²⁾ However, the rate constant of the beta-scission of the 1-hydroperoxy-3-propyl radical, produced by the isomerizations of a C_3 -alkylperoxy radical involving a six-membered ring transition state has been calculated using the quantum mechanics method. This reaction leads to the formation of ethylene, formaldehyde and a hydroxyl radical. The calculated rate constant is $k=6.8\times 10^{11}T^{0.551}\exp(-28100/RT)$ (in s^{-1} with R the gas constant in $\text{cal}\cdot\text{mol}^{-1}\cdot\text{K}^{-1}$). At 700 K, this value is 1.9 faster than the EXGAS rate constant.

All the above-described reactions (primary mechanism) produce stable molecules (primary products) for which consumption reactions need also to be written. The generation of these consumption reactions (secondary mechanism) is also automatically performed by EXGAS, but in the more globalized way than what is considered the primary mechanism, involving lumped species and globalized reactions.⁽³⁴⁾ In order to better represent the way of formation of some products, especially minor ones, we have revisited the reactions of C_3 hydroperoxides. These latter compounds are an important family of primary products of the oxidation of propane. The C_3 hydroperoxides produced during the oxidation of propane can be of two main types: propylhydroperoxides and C_3 hydroperoxides including a carbonyl group (ketohydroperoxides). Propylhydroperoxides are obtained from propylperoxy radicals by reaction with $\bullet\text{HO}_2$ radical. Ketohydroperoxides including a carbonyl group are obtained from peroxypropyl radicals by isomerization followed by a second addition to oxygen.

The decomposition of hydroperoxides occurs through the breaking of the O–O bond to form an alkoxy group and a hydroxyl radical. The rate constant is that proposed by Sahetchian et al.⁽³⁵⁾ Figures 8 and 9 present the different pathways which have been considered for the consumption of propylhydroperoxides and C₃ aldo-hydroperoxide, respectively. The latter species is the most important C₃ hydroperoxide including a carbonyl group since it is the only one formed through an isomerization involving six-membered ring transition states in the sequence of reactions producing degenerate branching agents.

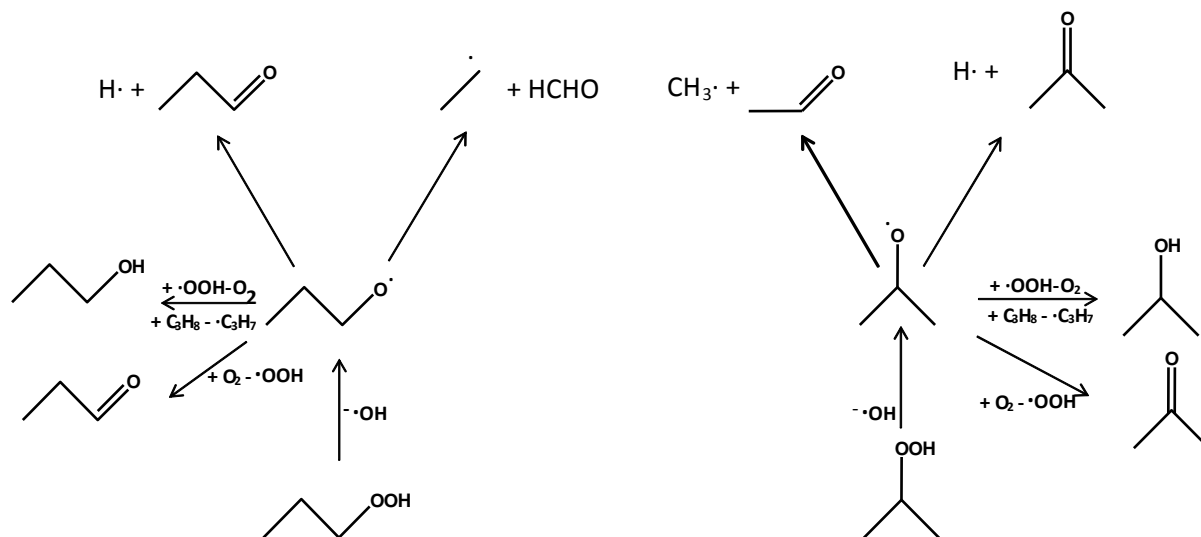


Figure 8. Detailed pathways considered for the decomposition of the propylhydroperoxides obtained from 1-propyl and 2-propyl radicals, respectively.

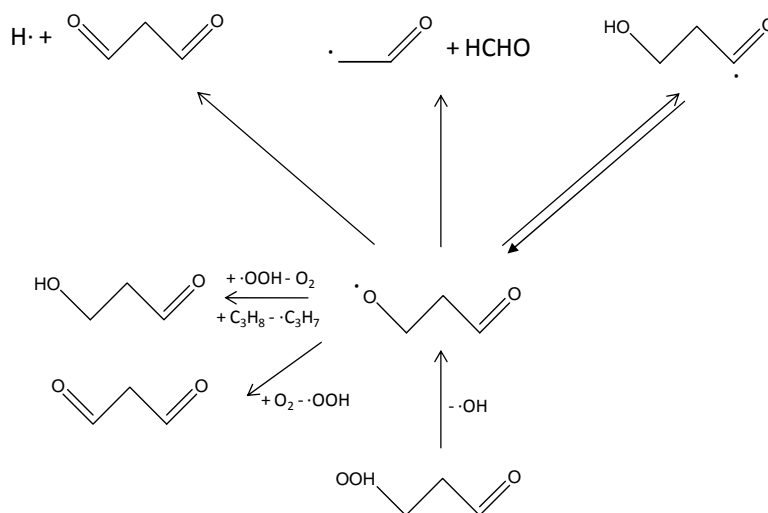


Figure 9. Pathways for the decomposition of aldo-hydroperoxide.

Five types of reaction are considered for the obtained saturated alkoxy or aldo-alkoxy radicals:

- The H-abstractions from propane to form alcohols with the same rate constants as that of the reactions of metathesis of propane by $\bullet\text{OH}$ radical, these values being much higher than the values for the reactions of metathesis of propane by $\text{CH}_3\text{O}\bullet$ radical.
- The disproportionation with $\bullet\text{HO}_2$ to also produce alcohols using the rate constant for a disproportionation between alkylperoxy and $\bullet\text{HO}_2$ radicals.⁽²²⁾
- The reactions with oxygen molecules to form a carbonyl function using the rate constant proposed by Atkinson et al.⁽³⁶⁾ for the primary alkoxy function and by Atkinson⁽³⁷⁾ for the secondary alkoxy function.
- The reactions of beta-scissions by breaking of a C–C bond yielding formaldehyde and CH_2CHO radicals or of a C–H bond giving propanedial.
- An isomerization, in the case of the aldo-alkoxy radicals.

The rate constants of the two last types of reactions have been calculated using the theoretical method previously described. Table 3 presents the kinetic parameters of these reactions, as well as a comparison with the rate constants calculated at the CBS-RAD and B3LYP/6-31G(d) level of theory by Rauk et al.⁽³⁸⁾ for the same reactions. Our rate constants are larger than those of Rauk et al.⁽³⁸⁾ by factors from 1.9 to 2.8 for C–C bond breaking, and by factors from 3.3 to 5.6 for C–H bond breaking.

Table 3. Kinetic Parameters Calculated for the Reactions of β -Scissions and Isomerizations Involved in the Decomposition of Alkoxy and Aldo-Alkoxy Species and Comparison with k_{Rauk} , the Values Proposed by Rauk et al.⁽³⁸⁾

$$k_{\infty} = AT^n \exp\left(-\frac{E}{RT}\right)$$

Reaction for which the calculation has been performed	Type of reaction	log (A×s)	n	E (kcal • mol ⁻¹)	k (s ⁻¹) at 700 K	k _{Rauk} (s ⁻¹) at 700 K
$\text{CH}_3\text{CH}_2\text{CH}_2(\text{O}\bullet) \rightleftharpoons \text{CH}_3\text{CH}_2\text{CHO} + \bullet\text{H}$	β -scission	10.8	1.04	19.8	$3.8 \cdot 10^7$	$6.7 \cdot 10^6$
$\text{CH}_3\text{CH}_2\text{CH}_2(\text{O}\bullet) \rightleftharpoons \text{CH}_3\text{CH}_2(\bullet) + \text{HCHO}$	β -scission	13.9	0.079	14.1	$5.3 \cdot 10^9$	$2.7 \cdot 10^9$
$\text{CH}_3\text{CH}(\text{O}\bullet)\text{CH}_3 \rightleftharpoons \text{CH}_3\text{COCH}_3 + \bullet\text{H}$	β -scission	11.4	0.77	17.9	$1.0 \cdot 10^8$	$3.0 \cdot 10^7$
$\text{CH}_3\text{CH}(\text{O}\bullet)\text{CH}_3 \rightleftharpoons \text{CH}_3\text{CHO} + \text{CH}_3\bullet$	β -scission	13.7	0.24	14.3	$8.3 \cdot 10^9$	$3.0 \cdot 10^9$
$\text{CH}_2(\text{O}\bullet)\text{CH}_2\text{CHO} \rightleftharpoons \text{CHOCH}_2\text{CHO} + \bullet\text{H}$	β -scission	11.3	0.97	22.1	$1.4 \cdot 10^7$	
$\text{CH}_2(\text{O}\bullet)\text{CH}_2\text{CHO} \rightleftharpoons \text{HCHO} + \text{CH}_2(\bullet)\text{CHO}$	β -scission	12.3	0.43	12.2	$5.2 \cdot 10^9$	
$\text{CH}_2(\text{O}\bullet)\text{CH}_2\text{CHO} \rightleftharpoons \text{CH}_2(\text{OH})\text{CH}_2\text{C}(\bullet)\text{O}$	isomerization	10.7	0.31	9.2	$5.1 \cdot 10^8$	

The carbonyl radical deriving from the isomerization of the aldo-alkoxy radicals has been considered to react either by an α -scission producing CO and $\text{C}_2\text{H}_4\text{OH}$ radicals, or by an addition to oxygen. The latter pathway is followed by a six-membered ring isomerization and a β -scission producing ethenol, carbon dioxide and a hydroxyl radical. The same type of reaction has been considered for the

aldocarbonyl radicals obtained by H-abstraction from propanedial, which is produced by disproportionation from aldo-alkoxy radicals. The rate constants of the reactions of carbonyl radicals have been evaluated based on the reactivity of $\text{CH}_3\text{CO}\bullet$ radicals obtained from acetaldehyde.

Primary and Secondary Mechanism of the Oxidation of Propene

The mechanism generated by EXGAS for the oxidation of propene contains unimolecular and bimolecular initiations, as well as H-abstractions to produce allyl radicals with kinetic data proposed by Heyberger et al.⁽²³⁾ It also contains the addition of small radicals on the double bond with kinetic data also from Heyberger et al., except in the case of $\bullet\text{OH}$ radical for which the values recently proposed by Zádor et al.⁽²⁵⁾ have been used. Note also that all the possible β -scission reactions of all the radicals which are produced are systematically considered by EXGAS with rate constants proposed by Heyberger et al.⁽²³⁾ The combinations and disproportionations of allyl radicals, especially the reaction with $\bullet\text{HO}_2$ radicals yielding allylhydroperoxide were also taken into account.⁽²³⁾

The kinetic data of the reactions of hydroxypropyl and hydroxyhydroperoxypropyl radicals with oxygen, as well as those for the second addition to oxygen, were derived from the values proposed for propyl radicals at 1 atm by DeSain et al.⁽⁴⁾ In the case of the formation of propenol and $\bullet\text{HO}_2$ radicals from oxidation reactions, we have calculated the contributions of the different types of abstracted H atoms. While the case is found for instance in 2-hydroxy-1-propyl radicals, DeSain et al.⁽⁴⁾ do not study the case of tertiary radicals for the addition of oxygen and of tertiary hydrogen for the eliminations of $\bullet\text{HO}_2$, so we used the values for secondary radical and secondary hydrogen, respectively.

The rate constants for the isomerizations of hydroxypropylperoxy radicals involving a transition state including 5 or 6 atoms, as well as the subsequent formation of hydroxy cyclic ethers have been calculated using the theoretical method previously described. Calculations were performed for the 10 reactions presented in Table 4, which are representative of the main reactions which can occur starting from the two hydroxypropylperoxy radicals that can be obtained by additions of $\bullet\text{OH}$ radicals to propene followed by addition to oxygen.

Among these reactions, there are isomerizations involving the internal transfer of an alkylic H atom and the formation of cyclic ethers, but also the reactions following the mechanism of Waddington.⁽²⁸⁾ Table 4 shows a comparison between the calculated rate constants for the studied hydroxyl radicals and those obtained from the structure-reactivity relationships used by EXGAS.⁽²³⁾ This comparison leads to the same trends as those observed by Cord et al.⁽⁵⁾ for the reactions of radicals deriving from alkyl radicals: i.e., there are large deviations between EXGAS and calculated values for the isomerizations involving a six-membered transition state cycle and for the formation of oxiranes. Note also that as in ref 5, the spin contamination is important for all the transition states involved in the formation of cyclic ethers. For reactions following the mechanism of Waddington, EXGAS correlations consider the same rate constant for the two reactions in Table 4, whereas calculated rate constants are very different (almost 1 order of magnitude), one being in good agreement with the EXGAS data. The reason for this difference is unknown, since the chemical processes seem to be similar in the two reactions. Sun et al.⁽³⁹⁾ have also used the CBS-QB3 method to calculate the rate constants of reactions following the mechanism of Waddington in the case of *iso*-butene considering

the stabilization of the obtained hydroperoxyalkoxy radicals. Figure 10 presents a comparison between the rate constants proposed by Sun et al.⁽³⁹⁾ and those displayed in Table 4. It shows that, despite similar methods have been used in both cases, the values of Sun et al.⁽³⁹⁾ are larger than ours by almost an order of magnitude. However it is interesting to note that a good agreement is obtained between our calculations and those of Sun et al.⁽³⁹⁾ for the ratio between the rate constants of the two channels.

Table 4. Kinetic Parameters Calculated for the Isomerizations of Hydroxyalkylperoxy Radicals, the Waddington Reactions, and the Formation of Cyclic Ethers Involved in the Mechanism of Propene and Comparison with the Data Used by EXGAS⁽²¹⁾

$$k_{\infty} = AT^n \exp\left(-\frac{E}{RT}\right)$$

Reaction for which the calculation has been performed	Type of reaction	log (A _∞ s)	n	E (kcal • mol ⁻¹)	k (s ⁻¹) at 700 K	k / k _{EXGAS} at 700 K
CH ₂ (OH)CH(OO•)CH ₃ ⇌ CH ₂ (OH)CH(OOH)CH ₂ •	isomerization	-2.81	4.53	26.4	6.8·10 ¹	2.2
CH ₂ (OH)CH(OO•)CH ₃ ⇌ CH(•)(OH)CH(OOH)CH ₃	isomerization	1.72	2.99	22.2	2.0·10 ³	2.9
CH ₃ CH(OH)CH ₂ (OO•) ⇌ CH ₃ C(•)(OH)CH ₂ (OOH)	isomerization	2.98	2.52	20.2	7.0·10 ³	2.3
CH ₃ CH(OH)CH ₂ (OO•) ⇌ CH ₂ (•)CH(OH)CH ₂ (OOH)	isomerization	4.38	2.17	20.2	1.8·10 ⁴	23
CH ₂ (OH)CH(OO•)CH ₃ ⇌ •OH + CH ₃ CHO + HCHO	Waddington's reaction	9.47	0.45	21.5	1.4·10 ⁴	15.2
CH ₃ CH(OH)CH ₂ (OO•) ⇌ •OH + CH ₃ CHO + HCHO	Waddington's reaction	9.18	0.54	24.5	1.2·10 ³	1.8
CH ₂ (OH)CH(OOH)CH ₂ • ⇌ 1 hydroxymethyloxirane + •OH	formation of cyclic ether	10.6	0.46	11.0	3.0·10 ⁸	201
CH(•)(OH)CH(OOH)CH ₃ ⇌ 1 hydroxy-2-methyloxirane + •OH	formation of cyclic ether	12.4	0.067	11.2	1.2·10 ⁹	801
CH ₃ C(•)(OH)CH ₂ (OOH) ⇌ 1 hydroxy-1-methyloxirane + •OH	formation of cyclic ether	13.2	-0.096	10.5	4.5·10 ⁹	3144
CH ₂ (•)CH(OH)CH ₂ (OOH) ⇌ 1 hydroxy-oxetane + •OH	formation of cyclic ether	12.4	-0.19	20.7	2.5·10 ⁵	0.37

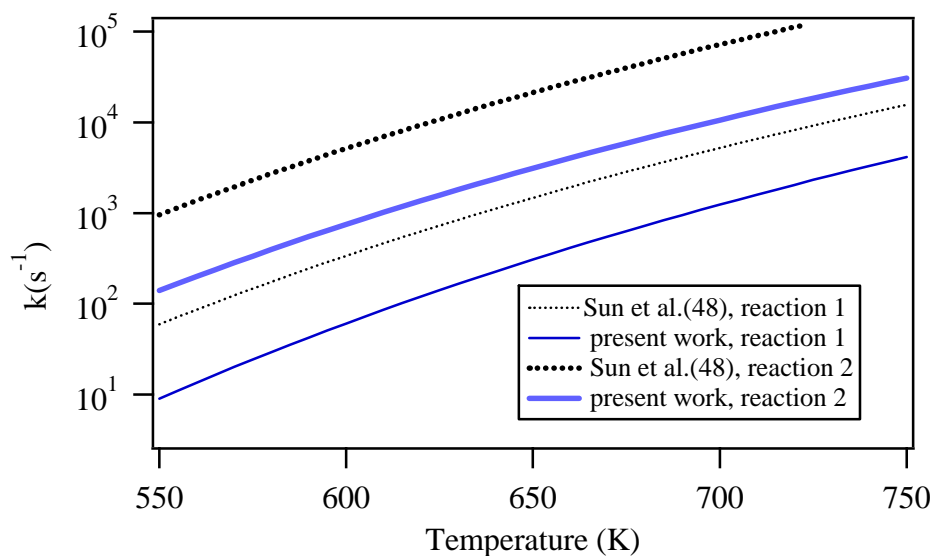


Figure 10. Comparison between the high pressure limit rate constants (k_{∞}) proposed in the present work and those of Sun et al.⁽³⁹⁾ for the 2 reactions involved in the mechanism of Waddington deriving from propene: reaction 1, $\text{CH}_3\text{C}(\text{R})(\text{OH})\text{CH}_2\text{OO}\cdot \rightleftharpoons \cdot\text{OH} + \text{CH}_3\text{C}(\text{R})\text{O} + \text{HCHO}$, with R being H in the present work and CH_3 in the work of Sun et al.⁽³⁹⁾ and reaction 2, $\text{CH}_3\text{C}(\text{R})(\text{OO}\cdot)\text{CH}_2\text{OH} \rightleftharpoons \cdot\text{OH} + \text{CH}_3\text{C}(\text{R})\text{O} + \text{HCHO}$.

Figure 11 presents a comparison between the rate constants of the different possible isomerization channels of hydroxypropylperoxy radicals. It shows that, contrary to the work of Sun et al.⁽³⁹⁾ in which the reactions following the mechanism of Waddington are always the preponderant ones, in the present study, it is only the case for the peroxy radicals with the alcohol function carried by the terminal atom of carbon. In the case of peroxy radicals with the alcohol function carried by the carbon atom in the middle, both possible isomerizations are the fastest channels.

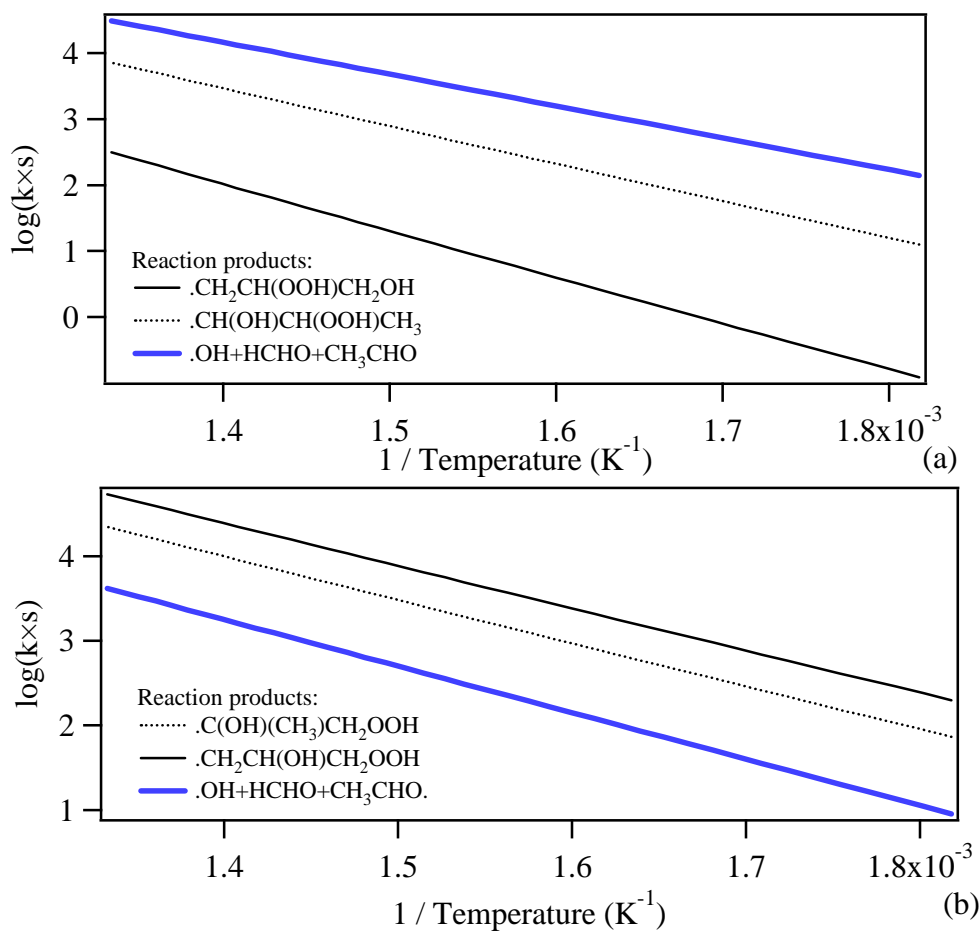
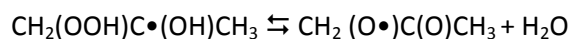


Figure 11. Comparison between the rate constants calculated for the different possible channels for the isomerizations of (a) $\bullet\text{OOCH(CH}_3\text{)CH}_2\text{OH}$ and (b) $\bullet\text{OOCH}_2\text{CH(OH)CH}_3$ radicals.

The rate constant of the β -scission for the 2-hydroxy-1-hydroperoxy-3-propyl radical produced by the isomerization of a C_3 -hydroxyalkylperoxy radical involving a six-membered ring transition state has also been calculated. This reaction leads to the formation of acetaldehyde, formaldehyde and a hydroxyl radical. The calculated rate constant is $k = 5.0 \times 10^{10} T^{0.172} \exp(-26300/RT) \text{ s}^{-1}$. At 700 K, this value is 23 slower than the EXGAS rate constant.

A specific decomposition giving a water molecule and an alkoxy radical has also been investigated for 2-hydroxy-1-hydroperoxy-2-propyl radical produced by the isomerizations of a hydroxypropylperoxy radical involving a five-membered ring transition state:



The rate constant of this decomposition involving a six-membered ring transition state has been calculated as equal to $k = 2.52 \times 10^{13} T^{-0.54} \exp(-14000/RT) \text{ s}^{-1}$ and shown to be 143 times lower at 700 K than the formation of oxirane which can also occur from 2-hydroxy-1-hydroperoxy-2-propyl radical. This reaction has then not been considered in the model. However, note that calculations

show that this type of decomposition could compete with the formation of cyclic ethers, especially oxetane formation, in the case of larger alkenes.

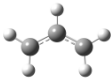
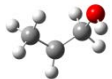


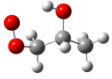
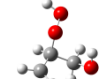

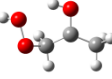
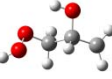
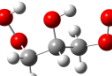
In the secondary mechanism, the reactions of the unsaturated alkoxy radicals deriving from allylhydroperoxide have been considered in more details. They can react by H-abstraction from propane with the same rate constants as that of the reactions of metathesis of propane by $\bullet\text{OH}$ radicals, or by β -scission by breaking of a C–C bond to give vinyl radicals and formaldehyde, or of a C–H bond yielding H atom and acrolein. The rate constants of these two last reactions were taken from Rauk et al.⁽³⁸⁾

Thermochemical Data

The major part of the thermochemical data for molecules or radicals considered in the present model have been calculated by the software THERGAS,⁽⁴⁰⁾ based on the group and bond additivity methods proposed by Benson,⁽⁴¹⁾ and stored as 14 polynomial coefficients, according to the CHEMKIN formalism.⁽⁴²⁾ However, at low-temperature, a small energy difference in thermochemical data can have a significant impact on the global reactivity as the kinetic parameters of the reverse reaction (for reversible reaction) are calculated from the ones of the direct reaction and from the thermodynamic properties of the species involved in the reaction. It is then important to use accurate thermochemical data, in particular for the reactions $\text{R} + \text{O}_2 = \text{ROO}$. Enthalpies of formation, entropies and heat capacities of the major C_3 radicals involved in the oxidation of propane and propene have been calculated by the quantum chemical methods described above.

The data related to propyl, propylperoxy, hydroperoxypropyl, and hydroperoxypropylperoxy radicals were already presented by Cord et al.⁽⁵⁾ Table 5 presents the calculated data for the C_3 hydroxy radicals of the four types at different temperatures, as well as a comparison with those obtained by group additivity methods using the THERGAS software.⁽⁴⁰⁾ As an example, the enthalpy of formation obtained for the allyl radical using THERGAS is deduced from the enthalpy of formation of propene (which is tabulated⁽⁴³⁾) and from the energy of the C–H bond which is broken to give the allyl radical (the energy of which is known⁽⁴⁴⁾). Table 5 shows that calculated enthalpies of formation are about $1 \text{ kcal}\cdot\text{mol}^{-1}$ lower for hydroxypropylperoxy radicals and about $2 \text{ kcal}\cdot\text{mol}^{-1}$ higher for hydroxyhydroperoxypropyl radicals compared to the values calculated by THERGAS.⁽⁴⁰⁾ Calculated entropies are about $3 \text{ cal}\cdot\text{K}^{-1}\cdot\text{mol}^{-1}$ lower for hydroxyalkylperoxy radicals and about $6 \text{ cal}\cdot\text{K}^{-1}\cdot\text{mol}^{-1}$ lower for hydroxyhydroperoxyalkyl radicals compared to the values calculated by THERGAS.⁽⁴⁰⁾ In THERGAS,⁽⁴⁰⁾ calculations do not take into account the effect of hydrogen bond hindering some rotations in the molecule.

Table 5. Enthalpies of Formation ($\text{kcal}\cdot\text{mol}^{-1}$), Entropies, and Heat Capacities ($\text{cal}\cdot\text{mol}^{-1}\cdot\text{K}^{-1}$) for the Allyl Radical and for C_3 Hydroxyalkyl, Hydroxyalkylperoxy, Hydroxyhydroperoxyalkyl, and Hydroxyhydroperoxyalkylperoxy Radicals, Calculated at the CBS-QB3 Level of Theory.^a In italics: data calculated using software THERGAS.⁽⁴⁰⁾

name	species	H_{298}	S_{298}	$C_{P,300}$	$C_{P,400}$	$C_{P,500}$	$C_{P,600}$	$C_{P,800}$	$C_{P,1000}$
allyl radical		39.5	63.0	14.9	18.8	22.0	24.7	28.8	31.8
		<i>40.7</i>	<i>61.6</i>	<i>14.6</i>	<i>18.3</i>	<i>21.5</i>	<i>24.2</i>	<i>28.6</i>	<i>31.8</i>
1-hydroxy-2-propyl radical		-14.2	80.0	21.2	25.4	29.3	32.7	38.1	42.2
		<i>-15.0</i>	<i>79.8</i>	<i>20.6</i>	<i>25.1</i>	<i>28.8</i>	<i>32.1</i>	<i>37.6</i>	<i>41.8</i>
2-hydroxy-1-propyl radical		-15.3	76.5	23.0	27.3	31.0	34.2	39.1	42.9
		<i>-16.4</i>	<i>77.5</i>	<i>21.2</i>	<i>26.4</i>	<i>30.6</i>	<i>34.0</i>	<i>39.3</i>	<i>43.1</i>
1-hydroxy-2-propylperoxy radical		-51.5	89.7	28.2	34.0	39.1	43.3	49.5	53.8
		<i>-50.6</i>	<i>92.2</i>	<i>27.3</i>	<i>33.3</i>	<i>38.3</i>	<i>42.4</i>	<i>48.4</i>	<i>52.7</i>
2-hydroxy-1-propylperoxy radical		-51.4	89.6	27.9	33.8	38.9	43.2	49.6	54.0
		<i>-50.6</i>	<i>92.2</i>	<i>27.3</i>	<i>33.3</i>	<i>38.3</i>	<i>42.4</i>	<i>48.4</i>	<i>52.7</i>
1-hydroxy-2-hydroperoxy-3-propyl radical		-34.6	92.5	30.6	36.6	41.7	45.8	51.6	55.5
		<i>-37.6</i>	<i>97.4</i>	<i>29.0</i>	<i>34.7</i>	<i>39.3</i>	<i>42.9</i>	<i>48.3</i>	<i>52.2</i>
1-hydroxy-2-hydroperoxy-1-propyl radical		-42.3	90.7	30.6	36.3	41.3	45.5	51.8	56.0
		<i>-42.8</i>	<i>97.5</i>	<i>28.8</i>	<i>34.4</i>	<i>38.7</i>	<i>42.3</i>	<i>47.7</i>	<i>51.7</i>
2-hydroxy-1-hydroperoxy-2-propyl radical		-42.9	91.9	29.2	35.0	40.3	44.7	51.2	55.6
		<i>-44.8</i>	<i>98.0</i>	<i>28.8</i>	<i>34.2</i>	<i>38.5</i>	<i>41.9</i>	<i>47.2</i>	<i>51.2</i>
2-hydroxy-1-hydroperoxy-3-propyl radical		-35.2	92.9	30.8	36.8	41.9	45.9	51.6	55.3
		<i>-36.9</i>	<i>98.7</i>	<i>29.0</i>	<i>34.7</i>	<i>39.3</i>	<i>42.9</i>	<i>48.3</i>	<i>52.2</i>
2-hydroxy-1-hydroperoxy-3-propylperoxy radical		-70.6	105.9	35.5	43.0	49.4	54.4	61.5	66.1
		<i>-70.7</i>	<i>111.6</i>	<i>34.9</i>	<i>41.7</i>	<i>47.2</i>	<i>51.6</i>	<i>57.8</i>	<i>61.9</i>

Reactions of C_0 – C_2 species

As in all EXGAS mechanisms,⁽²²⁾ a C_0 – C_2 reaction base as been added to the final mechanism of the oxidation of propane and propene in order to well consider the reactions of small species. This C_0 – C_2 reaction base includes all the reactions involving radicals or molecules containing less than three carbon atoms. The kinetic data used in the C_0 – C_2 reaction base were taken from the literature. The pressure dependent rate constants follow the formalism proposed by Troe⁽⁴⁵⁾ and efficiency coefficients have been included. As in our previous work about the oxidation of *n*-butane,⁽⁵⁾ the kinetic parameters of four reactions in the C_0 – C_2 reaction base have been up-dated: the rate constant proposed by Troe has been used for the reaction: $\text{H}_2\text{O}_2 (+\text{M}) \rightleftharpoons 2\cdot\text{OH} (+\text{M})$,⁽⁴⁶⁾ that proposed by You et al.⁽⁴⁷⁾ for the reaction $\text{CO} + \cdot\text{HO}_2 \rightleftharpoons \text{CO}_2 + \text{OH}\cdot$, that proposed by Vasudevan et al.⁽⁴⁸⁾ for the reaction $\cdot\text{OH} + \text{HCHO} \rightleftharpoons \text{H}_2\text{O} + \cdot\text{HCO}$, and that proposed by DeSain et al.⁽⁴⁾ for the reaction $\cdot\text{HCO} + \text{O}_2 \rightleftharpoons \text{CO} + \cdot\text{HO}_2$. The two following reactions, $\text{C}_2\text{H}_5\text{OO}\cdot + \text{CH}_3\text{OO}\cdot \rightleftharpoons \text{C}_2\text{H}_5\text{OH} + \text{HCHO} + \text{O}_2$ and $\text{C}_2\text{H}_5\text{OO}\cdot + \text{CH}_3\text{OO}\cdot \rightleftharpoons \text{CH}_3\text{OH} + \text{CH}_3\text{CHO} + \text{O}_2$, have been considered with the same rate constant as that of the disproportionation for two $\text{C}_2\text{H}_5\text{OO}\cdot$ radicals.

As acetic acid was not previously found among combustion intermediates, its reactions were not considered in the C₀–C₂ reaction base. In the present work, its formation has been considered from CH₃COOO• radical which is formed by O₂ addition to CH₃CO• radicals obtained from acetaldehyde by H atom abstractions. CH₃COOO• radical reacts then to give acetic acid by the following reactions: CH₃COOO• + CH₃OO• ⇌ CH₃C(O)OH + HCHO + O₂, and CH₃COOO• + •HO₂ ⇌ CH₃C(O)OH + O₂ + •O•. The rate constant of the first reaction is that proposed by Maricq et al.⁽⁴⁹⁾ The total rate constant of the reaction CH₃COOO• + •HO₂ and the branching ratio between the 2 possible channels giving either CH₃COOOH + O₂ (already considered in the C₀–C₂ reaction base), or CH₃C(O)OH + O₂ + •O• were taken from an experimental determination by Le Crâne et al.⁽⁵⁰⁾ The consumption of acetic acid has been described by pericyclic reactions, CH₃C(O)OH ⇌ CH₄ + CO₂, CH₃C(O)OH ⇌ CH₂CO + H₂O, and by H-abstraction by •OH radicals, CH₃C(O)OH + •OH ⇌ •CH₃ + CO₂ + H₂O. The rate constants of the first two reactions are from Duan et al.⁽⁵¹⁾ and the rate constant of the last reaction is from Huang et al.⁽⁵²⁾

Discussion

The complete mechanism (1159 reactions) described in this paper is available as Supporting Information. Simulations have been performed using the CHEMKIN software package.⁽⁴²⁾ Simulations for a jet-stirred reactor were performed assuming a homogeneous isothermal reactor and the computed profiles are shown in Figures 1, 2, and 5. The agreement between modeling and experimental results is very good for the profiles of the reactants with the temperature and the extent of the maximum of consumption being well simulated. The level of agreement is overall rather good for most of the reaction products, that is to say less than a factor 2. The shape and the position of the maximum of the profile of propylhydroperoxides is also well reproduced. More significant deviations are obtained in the cases of hydrogen peroxide, acetic acid, oxetane, acrolein, and 2-propen-1-ol. Note also that the formation of 1-hydroxy-2-propanone is not considered by the model, since its possible ways of formations are very uncertain.

The overprediction of the formation of hydrogen peroxide by a factor of 2.5 is due to the uncertainty on the photoionization cross-section of this compound, which is not available in literature and has then been roughly estimated. The overprediction of the formation of acetic acid is more difficult to explain since the same reactions of CH₃COOO• radicals have been used in recent models of the oxidation of *n*-butane⁽⁷⁾ and *n*-heptane⁽¹¹⁾ leading to a good simulation of this acid under experimental conditions very close to those of the present study. The only difference is that the hydrocarbon initial mole fractions were lower in our previous studies (0.04 for *n*-butane, and 0.005 for *n*-heptane instead of 0.12 here) since larger alkanes are more reactive fuels. We were not able to identify a second order reaction which can explain this discrepancy.

Figure 12 presents a flow rate analysis performed under the conditions of this study at 630 K and shows that propane reacts mainly by H-abstractions mostly with •OH radicals to give almost equal amounts of 1-propyl and 2-propyl radicals. Both radicals mostly react by addition to oxygen to form peroxy radicals, but about 15% of 2-propyl radical also yield propene by reaction with oxygen. The obtained propylperoxy radicals react by elimination of •HO₂ radical yielding propene (15% of the consumption of propyl-1-peroxy radical, and about 47% for propyl-2-peroxy radical), disproportionation with •HO₂ radicals to give alkylhydroperoxides (34% of the consumption of

propyl-1-peroxy radical, and about 20% for propyl-2-peroxy radical), and isomerizations to give hydroperoxypropyl radicals (44% of the consumption of propyl-1-peroxy radicals, and about 2% for propyl-2-peroxy radicals). A minor channel from propyl-2-peroxy radical also leads to the formation of acetone and a still smaller one yields propanal from propyl-1-peroxy radical (not shown in Figure 12).

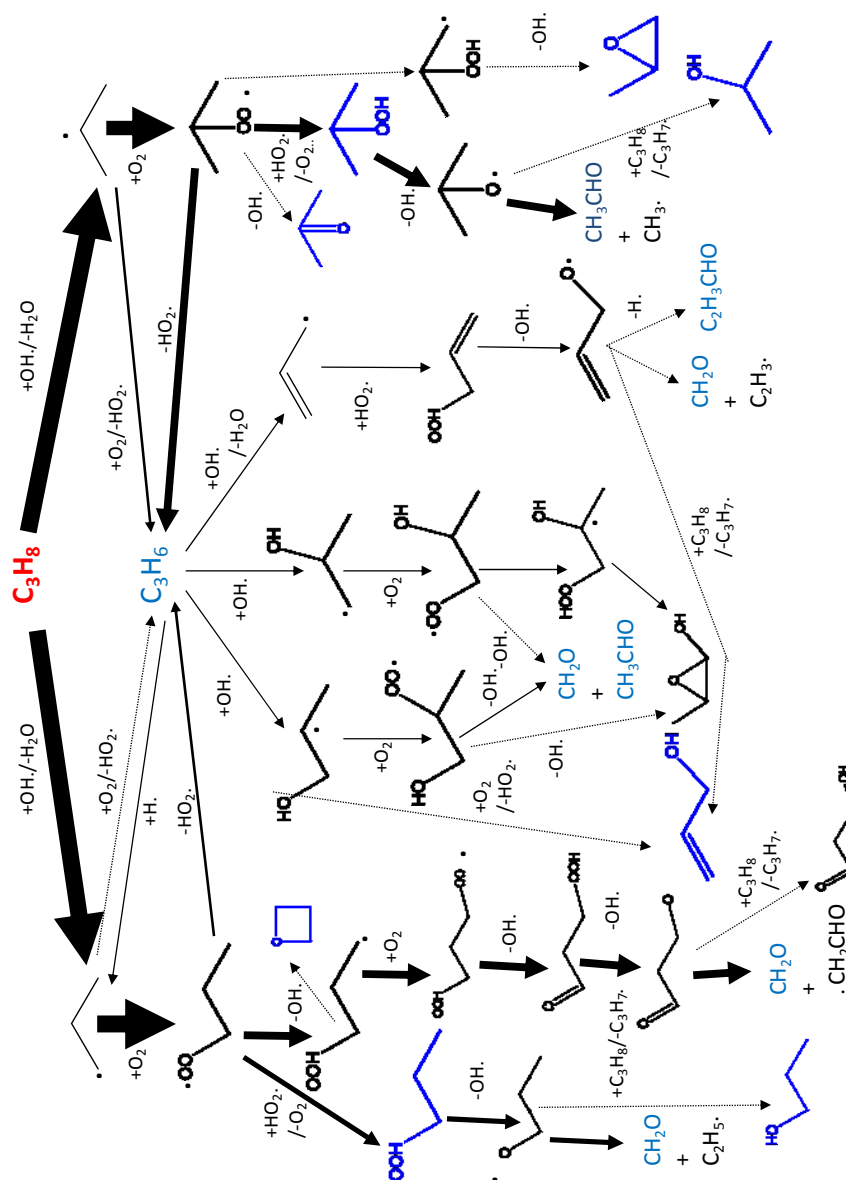


Figure 12. Flow rate analysis of the primary reactions of consumption of propane and propene under the conditions of Figure 1 at 630 K. The sizes of arrows are proportional to the net global fluxes and dotted arrows are for channels related to less than 3% of the propane consumption. Compounds in blue have been experimentally observed.

While only about 2% of propyl-2-peroxy radical yields hydroperoxypropyl radicals, this channel leads to the major cyclic ether obtained: methyloxirane, the formation of which is very well predicted. The

hydroperoxypropyl radicals formed from propyl-1-peroxy radicals react mainly by a second addition to oxygen and are a source of ketohydroperoxides. Only about 0.1% of these hydroperoxypropyl radicals lead to cyclic ethers, explaining the small formation of oxetane observed. The very large underprediction of this species is certainly due to the uncertainty in the calculated rate constant due to spin contamination as reported by Cord et al.⁽⁵⁾

Alkoxy radicals obtained by the decomposition of C₃ saturated hydroperoxides mostly react by breaking a C–C bond yielding formaldehyde with ethyl radicals, and acetaldehyde with methyl radicals. It is the main way of formation of acetaldehyde. Methyl and ethyl radicals are the main source of methane and ethylene, respectively. Oxirane derives from ethylene via reactions with methylperoxy and ethylperoxy radicals obtained also from methyl and ethyl radicals, respectively. Methanol is also obtained from methylperoxy radicals through the formation of methylhydroperoxide and CH₃O• radicals. The formation of both isomers of propanol also derives from these alkoxy radicals obtained via H-abstractions from propane. The prediction of these compounds has been shown to be very sensitive to the value of the rate constants used for the H-abstractions from propane. The used rate constants, which are those of the reactions of metathesis of propane by •OH radical, are much higher than the values for the reactions of metathesis of propane by CH₃O• radical and lead probably to an upper limit for the predicted formation of alcohols. Nevertheless when using the same values as in the case of methoxy radicals, almost no prediction of alcohols was observed.

Figure 13a displays the predicted mole fraction of the major C₃ ketohydroperoxide showing that it is lower by a factor 2 than that of propylhydroperoxides. This certainly does not fully explain why m/z 90 is not present in the measured mass spectra (see Figure 3), since its maximum fraction of 600 ppm should have been observed by SVUV-PIMS. The alkoxy radicals obtained by decomposition of the ketohydroperoxide deriving from propyl-1-peroxy radicals mostly decompose by breaking a C–C bond yielding formaldehyde. These aldo-alkoxy radicals are also a source of 3-hydroxypropanal through H-abstractions from propane. This last product, for which a mole fraction up to 20 ppm is computed (see Figure 13b), has not been observed experimentally. This discrepancy could both be due to a more difficult detection in GC analysis of compounds including 2 oxygenated functions and to uncertainties in the reactions deriving from ketohydroperoxides.

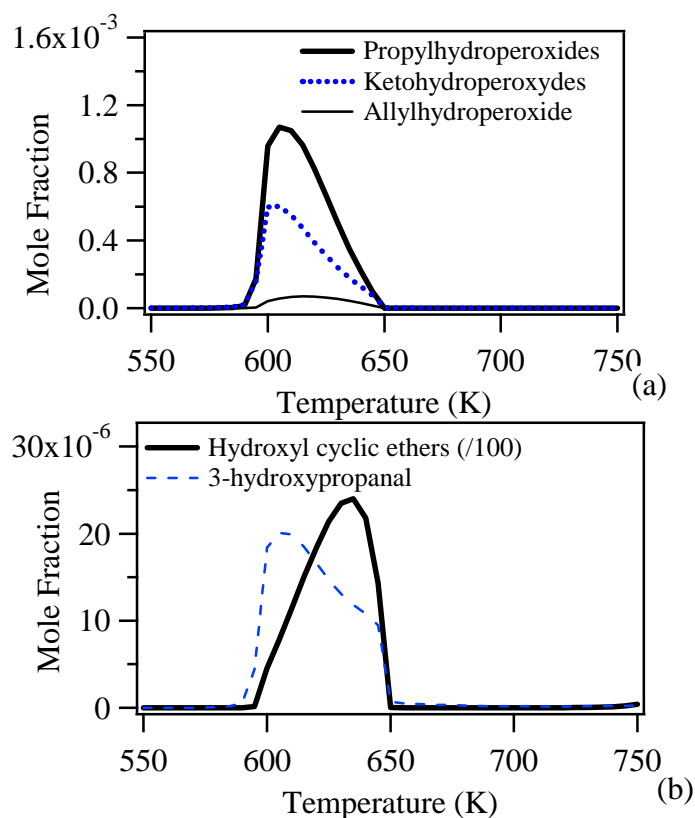


Figure 13. Simulated mole fraction of (a) the major hydroperoxides considered in the present mechanism and (b) hydroxyl cyclic ethers and 3-hydroxypropanal.

Compared to longer alkanes, a larger fraction of fuel (about 40%) is consumed to give the conjugated alkene, due to difficult isomerizations of small size peroxy radicals (the total isomerization rate constant at 700 K is equal to $5.0 \times 10^4 \text{ s}^{-1}$ for 1-peroxybutyl radical, and to $1.8 \times 10^4 \text{ s}^{-1}$ for 1-peroxypropyl radical). The fact that the formation of propene is well predicted supports the correctness of the values used for the rate constants of the reactions of propyl radicals with O_2 which were taken from the work of DeSain et al.⁽⁴⁾ At 630 K, under the conditions of Figure 12, the rate of consumption of propene is about 2/3 that of its production. Three ways of consumption of propene are important: the addition of H atoms to the double bond to give propyl radicals, the addition of $\bullet\text{OH}$ radicals yielding hydroxypropyl radicals, and H-abstractions producing mainly allyl radicals.

Hydroxypropyl radicals react with oxygen similarly to propyl radicals and are a source of propenol via reactions yielding $\bullet\text{HO}_2$ radicals, and of formaldehyde and acetaldehyde through the mechanism of Waddington, but also of hydroxyl cyclic ethers (mainly 2,3-methylhydroxyoxirane), which have not been observed experimentally, while a mole fraction up to 0.0025 (as shown in Figure 13b) is predicted. Note that 2,3-epoxycyclohexan-1-ol (but not 1,2-epoxycyclohexan-1-ol) has been observed during the oxidation of cyclohexene and would derive from the formation of $\bullet\text{OH}$ addition to cyclohexene.⁽⁵³⁾ The possibility of reactions of 2,3-methylhydroxyoxirane during the gas

chromatographic analyses leading to 1-hydroxy-2-propanol, a compound with a significant experimental mole fraction (see Figure 2) but no obvious way of formation in the model, cannot be excluded. Note that while the formation of $\bullet\text{QOOH}$ radicals is often neglected in models of the oxidation of alkenes in the literature, the formation rate through this channel in the case of 2-hydroxypropyl-1-peroxy radicals is much larger than that of its decomposition through the Waddington mechanism.⁽⁵⁴⁾

To show the influence of the reactions deriving from hydroxypropyl radicals, Figure 14 shows the results of a simulation using a model in which the additions of $\bullet\text{OH}$ radical on propene have been removed. It can be seen in this figure, that these reactions have only a very small effect on the global reactivity indicated by the consumption of propane, but a much more significant one on the formation of propene, acetaldehyde and acrolein.

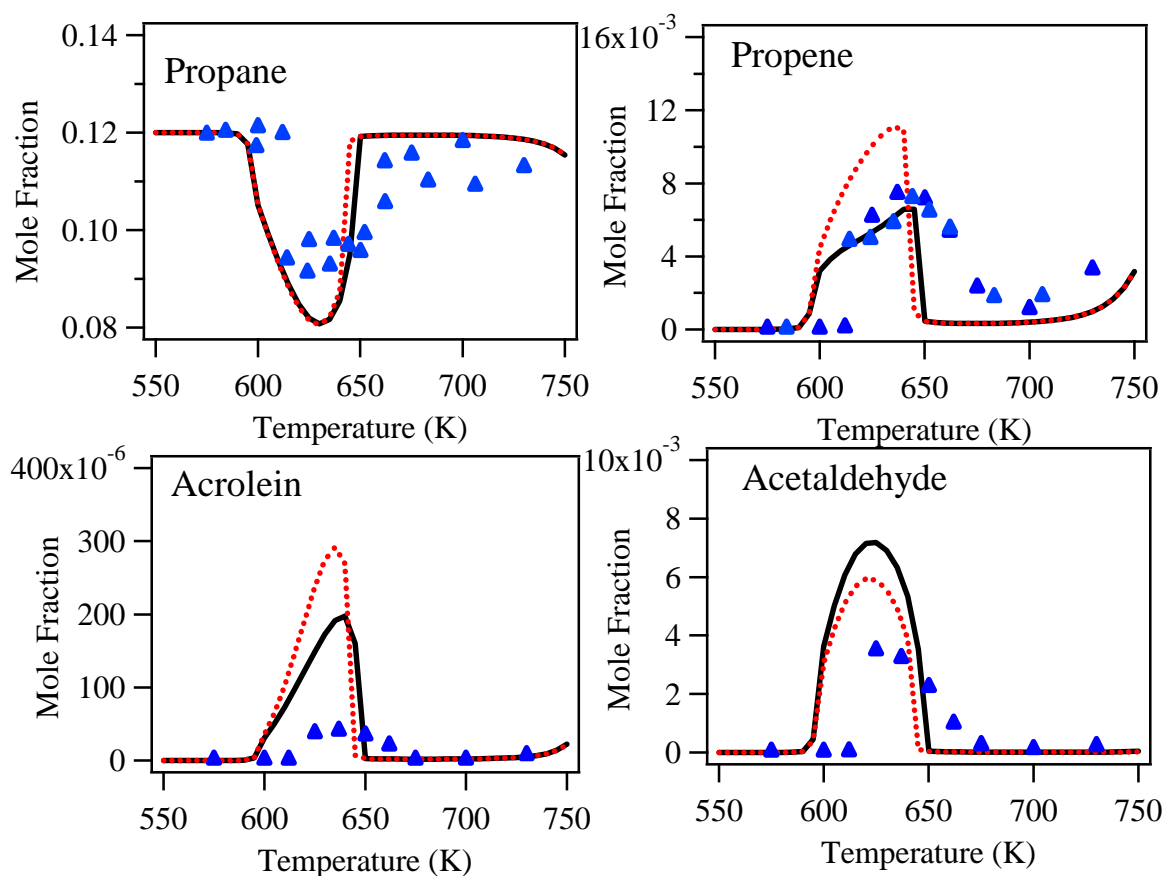


Figure 14. Influence of the addition of $\bullet\text{OH}$ radical on propene and subsequent reactions: the full lines correspond to a simulation with the full model and the dotted lines to simulations with removed $\bullet\text{OH}$ radical addition, and symbols are experiments as shown in Figures 1 and 2.

The main reaction of allyl radicals is by combination with $\bullet\text{HO}_2$ radicals to produce allylhydroperoxide which decompose yielding unsaturated alkoxy ($\text{C}_3\text{H}_5\text{O}\bullet$) and $\bullet\text{OH}$ radicals. $\text{C}_3\text{H}_5\text{O}\bullet$ radicals are an important source of acrolein and propenal. The strong overprediction of both products hints that

large uncertainties remain in the oxidation mechanism of allyl radicals. As shown in Figure 13a, the predicted mole fraction of allylhydroperoxide is much lower than those of propylhydroperoxides explaining probably why the peak at m/z 74 present in the measured mass spectra (see Figure 3) has rather been identified as 1-hydroxy-2-propanone in both sets of experiments. Also the maximum of formation of allylhydroperoxide occurs at slightly higher temperature than that of propylhydroperoxides and allylhydroperoxides showing well that allylhydroperoxide derives from reaction of propene, a product from propane.

Conclusion

The experimental study of the oxidation of propane was performed in a jet-stirred reactor and 21 reaction products were analyzed using two complementary methods: gas chromatography and SVUV photoionization mass spectroscopy. Theoretical calculations at the CBS-QB3 level of theory have been used to revisit the reactions involved in the low-temperature oxidation of propane and its important product, propene. A model has been proposed leading to satisfactory simulations of the global reactivity and of the formation of the main products. Note, however, that if the products directly deriving from propane through primary reactions are well simulated, the predictions are less good for species formed from propene or hydroperoxides. In particular, the reactions of allyl radicals still suffer of large uncertainties.

Supporting Information

Cartesian coordinates of the optimized structures of molecules, radicals, and transition states and complete mechanism of the low-temperature combustion of propane at 1 atm. This material is available free of charge via the Internet at <http://pubs.acs.org.bases-doc.univ-lorraine.fr>.

Acknowledgment

This work was supported by European Commission ("Clean ICE" ERC Advanced Research Grant) and by the COST Action CM0901. This work was granted access to the HPC resources of CINES under the allocation c2012086686 made by GENCI (Grand Equipement National de Calcul Intensif).

References

- (1) Battin-Leclerc, F. *Prog. Energ. Combust. Sci.*, **2008**, *34*, 440–498.
- (2) Vogin, B.; Baronnet, F.; Scacchi, G. *Can. J. Chem.-Rev. Can. Chim.* 1991, *69*, 43-61.
- (3) Koert, D. N.; Miller, D. L.; Cernansky, N. P. *Combust. Flame* 1994, *96*, 34-49.
- (4) DeSain, J.D.; Jusinski, L.E.; Andrew, A.D.; Taatjes, C.A. *Chem. Phys. Lett.* **2001**, *347*, 79-86.
- (5) Cord, M.; Sirjean, B.; Fournet, R.; Tomlin, A.; Ruiz-Lopez, M.; Battin-Leclerc, F. *J. Phys. Chem A*, **2012**, *116*, 6142-6158.
- (6) Zádor, J.; Jasper, A.W.; Miller, J.A. *Phys. Chem. Chem. Phys.*, **2009**, *11*, 11040-11053.
- (7) Herbinet, O.; Battin-Leclerc, F.; Bax, S.; Gall, H. L.; Glaude, P.-A.; Fournet, R.; Zhou, Z.; Deng, L.; Guo, H.; Xie, M.; Qi, F. *Phys. Chem. Chem. Phys.* 2011, *13*, 296-308.
- (8) Matras, D.; Villermaux, J. *Chem. Eng. Sci.* **1973**, *28*, 129-137.
- (9) Battin-Leclerc, F.; Blurock, E.; Bounaceur, R.; Fournet, R.; Glaude, P.-A.; Herbinet, O.; Sirjean, B.; Warth, V. *Chem. Soc. Rev.* **2011**, *40*, 4762-4782.
- (10) Husson, B.; Herbinet, O.; Glaude, P. A.; Ahmed, S. S.; Battin-Leclerc, F. *J. Phys. Chem. A* **2012**, *116*, 5100-5111.
- (11) Herbinet, O.; Husson, O.; Cord, M.; Fournet, R.; Glaude, P.A.; Sirjean, B.; Battin-Leclerc, F.; Wang, Z.; Xie, M.; Cheng, Z.; Qi, F. *Combust. Flame* **2012**, *159*, 3455-3471.
- (12) NIST Chemistry Webbook NIST Standard Reference Database 69 NIST, Gaithersburg, MD, 2005: <http://webbook.nist.gov/chemistry>.
- (13) Montgomery, J.A.; Frisch, M.J.; Ochterski, J.W.; Petersson, G.A. *J. Chem. Phys. A* **1999**, *110*, 2822-2827.
- (14) Frisch, M. J.; Trucks, G. W.; Schlegel, H. B.; Scuseria, G. E.; Robb, M. A.; Cheeseman, J. R.; Scalmani, G.; Barone, V.; Mennucci, B.; Petersson, G. A. et al. Gaussian 09, Revision B.01 Wallingford CT, 2009.
- (15) Arakawa, R., Mass spectral study of ionized-hydroxyacetone dissociation, *Bull. Chem. Soc. Jpn.*, 1991, *64*, 1022-1024.
- (16) Cool, T.A.; Mcllroy, A.; Qi, F.; Westmoreland, P.R.; Poisson, L.; Peterka, D.S.; Ahmed, M. *Rev. Sci. Instrum.* **2005**, *76* (9), 094102.
- (17) Cool, T.A.; Nakajima, K.; Mostefaoui, T.A.; Qi, F.; Mcllroy, A.; Westmoreland, P.R.; Law, M.E.; Poisson, L.; Peterka, D.S.; Ahmed, M. *J. Chem. Phys.* **2003**, *119* (16), 8356-8365.
- (18) Katayama, D.H.; Huffman, R.E.; Obryan, C.L. *J. Chem. Phys.* **1973**, *59* (8), 4309-4319.
- (19) Cooper, G.; Anderson, J.E.; Brion, C.E. *Chem. Phys.* **1996**, *209* (1), 61-77.
- (20) Chen, F.Z.; Robert Wu, C.Y. *J. Phys. B: At. Mol. Opt. Phys.*, **1999**, *32* (13), 3283-3293.
- (21) Warth, V., Stef, N., Glaude, P.A., Battin-Leclerc, F., Scacchi, G.; Côme, G.M. *Combust. Flame*, **1998**, *114*, 81-102.
- (22) Buda F.; Bounaceur R.; Warth V.; Glaude P.A.; Fournet R.; Battin-Leclerc F. *Combust. Flame*, **2005**, *142*, 170-186.
- (23) Heyberger, B.; Battin-Leclerc, F.; Warth, V.; Fournet, R.; Côme, G. ; Scacchi, G. *Combust. Flame*, **2001**, *126*, 1780-1802.
- (24) Touchard, S.; Fournet, R.; Glaude, P. A.; Warth, V.; Battin-Leclerc, F.; Vanhove, G.; Ribaucour, M.; Minetti, R. *Proc. Combust. Inst.* **2005**, *30*, 1073-1081.
- (25) Zádor, J.; Taatjes, C. A.; Fernandes, *Prog. Energ. Combust. Sci.*, **2011**, *37*, 371-421.
- (26) Walker R.W.; Morley C. In *Comprehensive Chemical Kinetics: low-temperature combustion and autoignition*, Pilling M.J. Ed., 35, Elsevier, Amsterdam, 1997.
- (27) Miller, J.A.; Pilling, M.J.; Troe, J. *Proc. Combust. Inst.* **2005**, *30* 43-88.
- (28) Pitzer, K.S.; Gwinn, W.D. *J. Chem. Phys.*, **1942** *10*, 428-440.
- (29) Mokrushin, V.; Tsang, W. Chemrate v.1.5.2; NIST, Ed. Gaithersburg, MD 20899, U.S.A., 2006.
- (30) Eckart, C. *Phys. Rev.* **1930**, *35*, 1303-1309.
- (31) Stark, M.S., Waddington, R.W. *Int. J. Chem. Kin.* **1995**, *27*, 123–51.

- (32) DeSain, J. D.; Klippenstein, S. J.; Miller, J. A.; Taatjes, C. A. *J. Phys. Chem. A* **2003**, *107*, 4415-4427.
- (33) Sharma, S.; Raman, S.; Green, W. H. *J. Phys. Chem. A* **2010**, *114*, 5689-5701.
- (34) Biet, J.; Hakka, M. H.; Warth, V.; Glaude, P.-A.; Battin-Leclerc, F. *Energ. Fuels* **2008**, *22*, 2258-2269.
- (35) Sahetchian, K.A., Rigny, R., Tardieu de Maleissye, J., Batt, L., Anwar Khan, M., Matthews, S. *Symp. Int. Combust.* **1992**, *24*, 637-643.
- (36) Atkinson, R., Baulch, D.L., Cox, R.A., Crowley, J.N., Hampson, R.F, Jr., Kerr, J.A., Rossi, M.J., Troe, J. IUPAC Subcommittee on Gas Kinetic Data Evaluation for Atmospheric, Chemistry Web Version December 2001 1-56
- (37) Atkinson, R. *Int. J. Chem. Kinet.* **1997**, *29*, 99-111.
- (38) Rauk, A.; Boyd, R.J.; Boyd, S.L.; Henry, D.J.; Radom, L. *Can. J. Chem.* **2003**, *81* 431-442.
- (39) Sun, H.; Bozzelli, J.; Law, C.K. *J. Phys. Chem. A* **2007**, *111*, 4974-4986.
- (40) Muller, C.; Michel, V.; Scacchi, G.; Côme, G.M., *J. Chim. Phys.*, **1995**, *92*, 1154-1178.
- (41) Benson, S.W., *Thermochemical Kinetics*, 2nd ed., John Wiley, New York, 1976.
- (42) Kee, R.J., Rupley, F.M.; Miller, J.A., Sandia Laboratories Report, SAND 89-8009B, 1993.
- (43) Furuyama, S., Golden, D.M., Benson, S.W., *J. Chem. Thermodyn.*, **1969**, *1*, 363-375.
- (44) Tsang, W., *Heats of Formation of Organic Free Radicals by Kinetic Methods in Energetics of Organic Free Radicals*, Martinho Simoes, J.A.; Greenberg, A.; Liebman, J.F., eds., Blackie Academic and Professional, London, 1996, 22-58.
- (45) Troe, J., *Ber. Buns. Phys. Chem.* **1974**, *78*, 478.
- (46) Troe, J. *Combust. Flame*, **2011**, *158*, 594-601.
- (47) You, X., Wang, H., Goos, E., Sung S.J., Klippenstein, S.J. *J. Phys. Chem. A* **2007**, *111*, 4031-4042.
- (48) Vasudevan, V., Davidson, D.F., Hanson, R.K. *Int. J. Chem. Kin.* **2005**, *37*, 99-109.
- (49) Maricq, M.M., Sente, J.J. *J. Phys. Chem.* **1996**, *100*, 4507-1513.
- (50) Le Crâne, J.P., Rayez, M.T., Rayez, J.C., Villenave, E. *Phys. Chem. Chem. Phys.* **2006**, *8*, 2163-2171.
- (51) Duan, X., Page, M. *J. Am. Chem. Soc.* **1995**, *117*, 5114 – 5119.
- (52) Huang, Y.W., Dransfield, T.J., Miller, J.D., Rojas, R.D., Castillo, X.G., Anderson, J.G. *J. Phys. Chem. A* **2009**, *113*, 423-430.
- (53) Ray, A.M.; Taatjes, C.A.; Welz, O.; Osborn, D.L.; Meloni, G. *J. Phys. Chem. A* **2012**, *116*, 6720-6730.
- (54) Mehl, M.; Vanhove, G.; Pitz, W. J.; Ranzi, E. *Combust. Flame* **2008**, *155*, 756-772.